TIGER TIDAL STREAM INDUSTRY ENERGISER

EUROPEAN UNION
European Regional Development Fund

T1.6.6 Deliverable:

Technical report on high-fidelity flow data field work and analysis, including vessel-based flow measurements and turbulence measurements at MeyGen

V1

June 2023

Interreg France (Channel Manche) England
European Regional Development Fund

TIGER TIDAL STREAM INDUSTRY ENERGISER

EUROPEAN UNION
European Regional Development Fund

Funding

This work was delivered by the Tidal Stream Industry Energiser project (TIGER) and was co-financed by the European Regional Development Fund through the Interreg France (Channel) England Programme.

Document History

Revision	Date	Description	Originated by	Reviewed by	Approved by
1	June 2023	Final	SA	DB	DB

Disclaimer

TIDAL STREAM INDUSTRY ENERGISER

EUROPEAN UNION
European Regional Development Fund

Contents

1 Introduction 1

1 Introduction

The “MEY-21-2-REP-001-F-MeyGen- 2022 Field Work Analysis Report_Rev2” report below summarises the outcomes of high-fidelity flow data field work and data analysis undertaken at the MeyGen site in 2022-2023.

This work was undertaken in the TIGER project in order to develop, and practically test at a key tidal stream site (MeyGen, UK), the development of a novel approach to collecting flow data at multiple potential future tidal turbine locations which could be robust enough for large-scale tidal stream array development/optimisation.

This novel approach has the potential to provide more accurate flow data for the development of large-scale tidal stream arrays than current industry-standard approaches which are mainly based on hydrodynamic modelling. As accurate flow data is a key parameter for design purposes and for energy yield analysis, the novel approach is of significant interest to Normandie Hydroliennes for the development of its tidal stream project at Raz Blanchard, France, as well as the wider tidal stream sector.

MeyGen has approached the IEC TS 62600-201 maintenance team to discuss its findings from the work, and the approach is planned to be incorporated into future editions of the IEC TS 62600-201 technical specification.

As part of the field work involved the collection of high-fidelity turbulence data from seabed-mounted 5-beam ADCP measurements, and it is highly beneficial for the tidal stream industry to have more public domain information on turbulence from such deployments, these turbulence results are also presented – together with an analysis of how the results differ when using a 4-beam and 5-beam method.

The field work also involved the collection of high-fidelity flow data from vessel-mounted ADCP measurements to assess the wakes from operational turbines. As there is very limited public domain information on tidal stream turbine wakes from operational turbine deployments, these results are also presented.

Normandie Hydroliennes hopes, and anticipates, that this publication will assist the whole tidal stream industry as it develops larger-scale arrays.

Technical report on high-fidelity flow data field work and analysis, including vessel-based flow measurements and turbulence measurements

This technical report summarises the outcomes of high-fidelity flow data field work and data analysis undertaken at the MeyGen site in 2022-2023.

F. Johnson

Author: F. Johnson	Document No: MEY-21-2-REP-001-F-Meygen- 2022 Field Work Analysis Report.Docx	Revision: 2

Document Title:

Technical report on high-fidelity flow data field work and analysis, including vessel-based flow measurements and turbulence measurements

Document History and Status

Revision	Approved by (internally)	Date approved	Date issued	Comment
1	D. Taaffe	28/03/2023	28/03/2023	First draft for OREC comment
2	D. Taaffe	16/06/2023	16/06/2023	Final

26 Dublin Street,
Edinburgh,
United Kingdom,
EH3 6NN
www.meygen.com

Contents

1 INTRODUCTION 2

2 HIGH-FIDELITY SMADCP MEASUREMENTS AND DATA ANALYSIS 3

2.1 Turbulence 3

2.1.1 Filtering 4

2.1.2 Results 5

2.1.2.1 TI vs current magnitude for various heights above seabed 5

2.1.2.2 TI profile with height above seabed 8

2.1.2.3 TI using 4-beam method vs. 5-beam method 9

2.1.2.4 TKE profile with height above seabed 12

2.1.2.5 TI using 4-beam method vs. 5-beam method 13

3 HIGH-FIDELITY VMADCP MEASUREMENTS AND DATA ANALYSIS 14

3.1 Stationary data collection trials 15

3.2 Stopover data collection trials 15

3.3 Wake drift measurement results 17

3.4 Wake drive-up measurement results 18

3.5 Wake transect measurement results 19

3.5.1 Assessment of the required number of repeat wake transects 20

3.5.2 Results from repeated wake transects 21

3.6 Wake stopover measurement results 24

3.7 Resource assessment using combined stopover VMADCP and SMADCP data... 24

3.7.1 Time lag investigation 25

3.7.2 VMADCP vs SMADCP correlation at SMADCP location 25

3.7.2.1 Data selection 25

3.7.2.2 Data analysis 26

3.7.2.3 Results 26

3.7.3 VMADCP vs SMADCP correlation at potential turbine locations 27

3.7.3.1 Results 27

3.7.3.2 Conclusions 29

Figure 1 – Axis conventions ... 4
Figure 2 - Average profiles of 50th, 90th and 99th TI percentiles for conditions with current magnitude > 1 m/s when Hm0 < 0.5 m (rounds, solid line) and for all sea states (stars, dotted line) ... 5
Figure 3 - 50th, 90th and 99th percentiles of TI along X_L axis ... 6
Figure 4 - 50th, 90th and 99th percentiles of TI along Y_L axis ... 7
Figure 5 - 50th, 90th and 99th percentiles of TI along Zup axis ... 8
Figure 6 - 50^{th}, 90^{th} and 99^{th} TI percentiles along X_L, Y_L and Z_{up} axes through the water column, for currents > 1m/s ... 9
Figure 7 - Scatter plots of TI in the X_L direction using 5-beam equations against 4-beam equations for reference heights above seabed ... 10
Figure 8 - Scatter plots of TI in the Y_L direction using 5-beam equations against 4-beam equations for reference heights above seabed ... 11
Figure 9 - Scatter plots of TI in the Z_{up} direction using 5-beam equations against 4-beam equations for reference heights above seabed ... 12
Figure 10 - Turbulence kinetic energy profiles split per percentile ... 13
Figure 11 - Scatter plots of TKE established using 5-beam equations against 4-beam equations for reference heights above seabed ... 14
Figure 12 - Definition of area around TTG4 used in the data analysis ... 16
Figure 13 - VMSDCP and TMADCP data comparison for TTG4 stopover trial ... 16
Figure 14 – Wake drift on TTG3 ... 17
Figure 15 – Wake drift on TTG3 ... 17
Figure 16 – Wake drift on TTG4 ... 18
Figure 17 – Wake drift on TTG4 ... 18
Figure 18 – Wake drive-up (ebb tide) ... 19
Figure 19 – Wake drive -up (flood tide) ... 19
Figure 20 – Downstream velocity estimates from repeated transects in turbine wake ... 20
Figure 21 – Downstream velocity convergence from repeated transects in turbine wake ... 21
Figure 22 – Scaled downstream velocity, flood direction (turbine off) ... 22
Figure 23 – Scaled downstream velocity, flood direction (turbine on) ... 22
Figure 24 – Scaled downstream velocity, ebb direction (turbine off) ... 23
Figure 25 – Scaled downstream velocity, ebb direction (turbine on) ... 23
Figure 26 – Downstream velocity deficit, ebb direction (turbine on) ... 23
Figure 27 – Scaled velocity magnitude and direction at +10D (ebb) ... 24
Figure 28 – Scaled velocity magnitude and direction at +14D (flood) ... 24
Figure 29 – Vessel tracks for VMADCP data over SMADCP location and target location ... 26
Figure 30 – Linear regression of VMADCP vs SMADCP data at 19m below LAT (stationary data) ... 27
Figure 31 – Linear regression of VMADCP vs SMADCP data for rotor disk (stationary data) ... 27
Figure 32 – Linear regression of VMADCP vs SMADCP data for rotor disk (stopover data) ... 28
Figure 33 – Linear regression of VMADCP vs SMADCP data for rotor disk (stopover data) ... 28

Abbreviations

ADCP	Acoustic Doppler Current Profiler
SMADCP	Seabed-mounted ADCP
TMADCP	Turbine-mounted ADCP
VMADCP	Vessel-mounted ADCP
IEC	International Electrotechnical Commission
LAT	Lowest Astronomical Tide
mab	Metres above (sea)bed

1 INTRODUCTION

This technical report summarises the outcomes of high-fidelity flow data field work and data analysis undertaken at the MeyGen site in 2022-2023.

This work included:

1. Development of a novel approach to collect flow data at potential future tidal turbine locations (as further detailed below and using (2) and (3)), which could be robust enough for array development/optimisation whilst potentially avoiding the need to undertake the currently industry-standard approaches outlined below, as recommended in IEC TS 62600-201[1]:

    a. deploy a Seabed-Mounted ADCP (SMADCP) for c. 90 days at each potential future tidal turbine location (financially unviable for arrays larger than a few turbines, intended for < 10MW arrays);

    b. rely on hydrodynamic modelling outputs with calibration and validation from c. 35 day SMADCP deployments (with an uncertainty which is difficult to quantify, especially for larger arrays and/or arrays which cover a relatively large area and/or where the resource changes significantly across the array area).

2. High-fidelity SMADCP measurements and the associated data analysis. This was to provide high-fidelity turbulence data for an area of the MeyGen site distant from the currently deployed 4-turbine array, and to provide an accurate current velocity to which other concurrent Vessel-Mounted ADCP (VMADCP) measurements could be correlated. Detailed results are included in this report to add to the industry knowledge of turbulence at different sites.

3. High-fidelity VMADCP measurements and the associated data analysis. This was to:

    a. undertake measurements of wake development and dissipation from existing MeyGen turbines to allow the industry to calibrate and validate mathematical modelling of an operational turbine wake;

    b. undertake measurements at potential future tidal turbine locations for array development/optimisation, based on the approach developed in (1).

The novel approach outlined in (1) was initially hypothesised in order to address the issues stated in (1), and then developed based on an analysis of existing measurements and hydrodynamic modelling of the MeyGen site. This provided a basis for the further refinement of the approach, which was then later used in practice.

The approach uses VMADCP data collected from an almost-stationary ‘stopover’ at a proposed turbine location and correlating the resultant stopover data to the concurrently-collected data (later retrieved) from a nearby SMADCP.

The method was initially tested for the ability of a relatively standard (non-moored, non-dynamically positioning) fast-response/crew transfer/safety vessel to remain almost-stationary in the highly turbulent and fast currents at the MeyGen site, and whether suitably robust VMADCP data could be collected. After these practical trials, the main survey work used c. 5-7 minute stopovers at potential turbine locations every hour during spring tides. The various potential turbine locations were split into separate days, with some overlap, as the maximum number of potential turbine locations that can be measured in each 12 hour period is restricted by the requirement to return to each potential turbine location every hour. This stopover data was correlated to the concurrent SMADCP data, and that correlation then used to predict the flow occurrence at each turbine location.

[1] Marine energy – Wave, tidal and other water current converters – Part 201: Tidal energy resource assessment and characterization. Edition 1.0. 2015-04. https://webstore.iec.ch/preview/info_iec62600-201%7Bed1.0%7Den.pdf

The remainder of this report focusses on items (2) and (3), which together encapsulate the novel approach intended to overcome the issues noted in item (1).

MeyGen contracted Applied Renewables Research Ltd. (ARR) to supply the ADCPs for the survey work and to undertake key aspects of the ADCP surveys and the analysis of the resulting data; key aspects of the analysis were contracted to DynamOcean EURL (DO). MeyGen contracted the vessels required for the work separately.

The majority of the information presented in the following sections is drawn directly from the associated ARR/DO reports, which are acknowledged here in their entirety and not referenced/acknowledged on each occasion.

2 HIGH-FIDELITY SMADCP MEASUREMENTS AND DATA ANALYSIS

The high-fidelity SMADCP results are based on a 5-beam SMADCP measurement campaign (using an RDI Sentinel V) which was 42 days in total, of which 41 days were used for the analysis of mean currents and waves, and 37 days for the analysis of turbulence. The 41 days for the analysis of mean currents exceeds an IEC TS 62600-201 (35 day) requirement (as outlined in Section 1).

SMADCP measurements were sampled at 2Hz, with 600s ensembles and 1080 pings per ensemble, and consist of:

- Pitch, Roll, Heading;
- Pressure;
- Profiles along the 5 beams, with 1m depth cell bin size, of:
    - Beam velocities;
    - Echo-intensity (or amplitude);
    - Correlation.

Key aspects of note are:

- Pitch and roll fluctuated at c. -1° and c. 1° respectively. Tilt standard deviation was mostly below 0.2°. Mean heading is approximately 90° with standard deviation lower than 0.6°.
- The beam correlation, echo intensity, and beam velocities all show satisfactory data.
- All IEC TS 620600-201 requirements relevant to SMADCP deployments were met or exceeded.

The SMADCP measurements were used to provide an accurate current velocity to which other concurrent VMADCP measurements could be correlated, as discussed in Section 0. For simplicity, these results are reported in Section 3.

The other main parameters of interest, as reported in the next section, are related to high-fidelity turbulence.

2.1 Turbulence

Turbulence is described in terms of Reynolds stresses, turbulence intensities (TI) and turbulent kinetic energy (TKE).

The normal Reynolds stresses $\overline{u'^2}$, $\overline{v'^2}$ and $\overline{w'^2}$ are calculated from beam velocity variances using equations 129, 130 and 131 in Dewey and Stringer 2007[2]. The TKE and TI are then derived from the Reynolds stresses:

$$TKE \equiv \frac{q^2}{2} = \frac{\left(\overline{u'^2} + \overline{v'^2} + \overline{w'^2}\right)}{2} \qquad TI = \frac{\sqrt{\frac{2q^2}{3\ 2}}}{U},\ TI_x = \frac{\sqrt{\overline{u'^2}}}{U},\ TI_y = \frac{\sqrt{\overline{v'^2}}}{U},\ TI_z = \frac{\sqrt{\overline{w'^2}}}{U}$$

Where U is the magnitude of the mean horizontal velocity.

The ADCP Y_L axis is within c. 6 degrees of the channel X_{ch} axis which allows the horizontal TI_X and TI_Y values within levelled instrument coordinates to be used as proxies for the estimates in channel axes coordinates, see Figure 1.

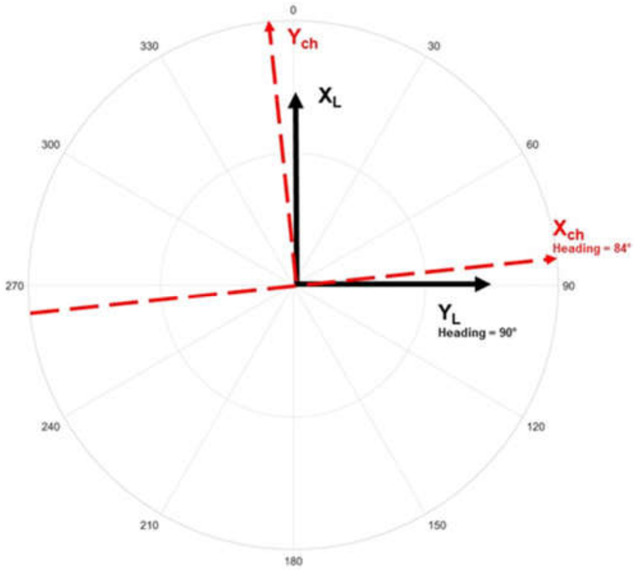

Figure 1 – Axis conventions

2.1.1 Filtering

After estimation and removal of Doppler noise, followed by filtering out conditions in which large waves (H_{m0} > 0.5 m) were recorded, turbulence parameters were generated. H_{m0} has been used as a filter to minimise wave influence; see Figure 2 for a comparison of TI metrics with and without the filter applied. Most of the filtering of larger sea states was over a period of c. 9 days when a large storm passed through the site; the majority of this was during neap tides.

A comparison of TI metrics between filtered and unfiltered data sets showed that the wave filtering process applied was effective.

[2] Dewey, R., & Stringer, S. (2007). Reynolds Stresses and Turbulent Kinetic Energy Estimates from Various ADCP Beam Configurations: Theory. Journal of Physical Oceanography, 35.

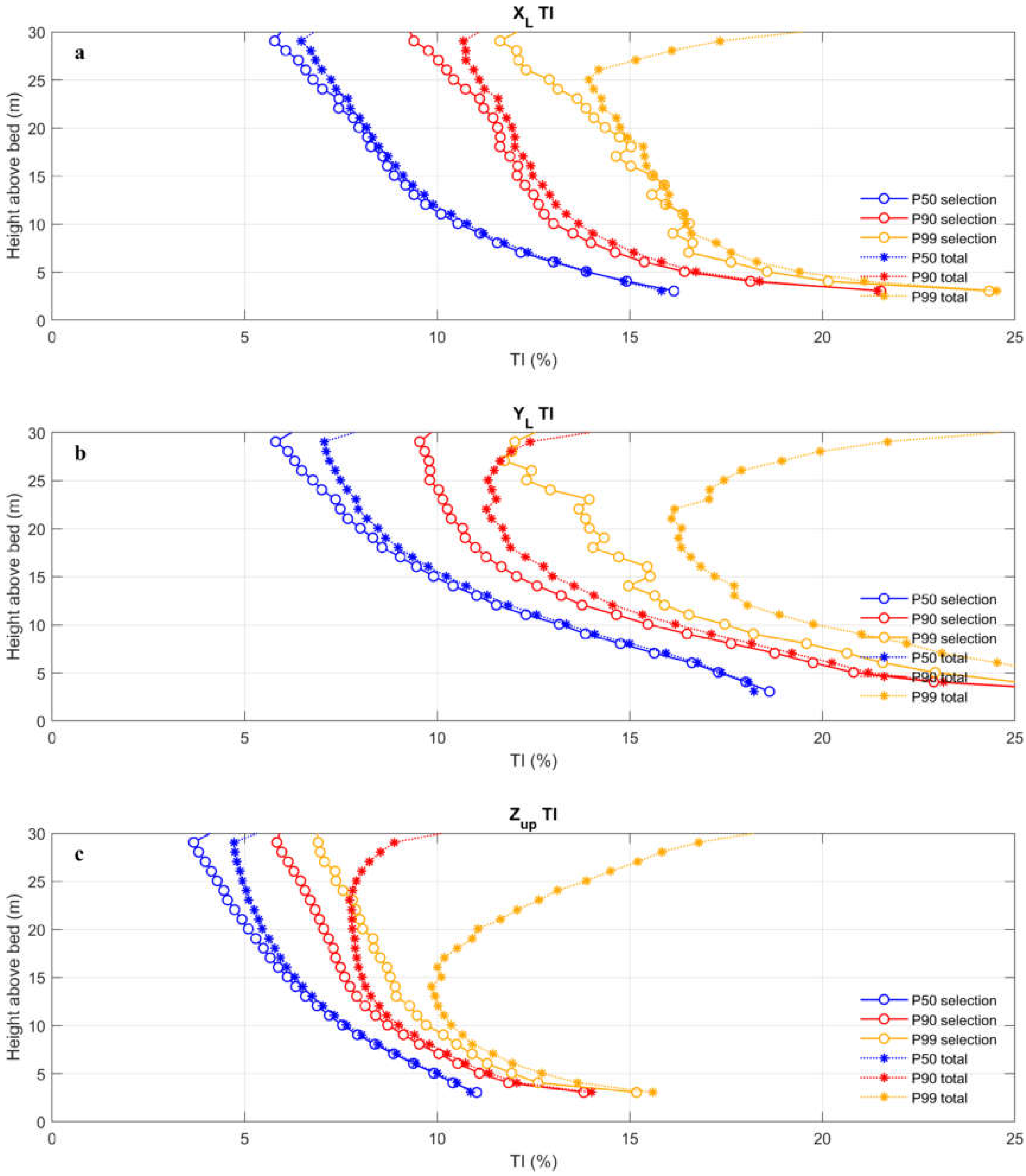

Figure 2 - Average profiles of 50th, 90th and 99th TI percentiles for conditions with current magnitude > 1 m/s when Hm0 < 0.5 m (rounds, solid line) and for all sea states (stars, dotted line)

2.1.2 Results

2.1.2.1 TI vs current magnitude for various heights above seabed

Figure 3 to Figure 5 show the P50, P90 and P99 values of TI in levelled-instrument coordinates X_L, Y_L and Z_{up}, as a function of signed current velocity magnitude and height above the seabed (mab). P50, P90 and P99 were derived based on the mean and standard deviation of TI for each velocity class.

TI results show a tidal asymmetry, with TI values being larger during flood tides (positive signed velocity magnitude). This effect is more visible at the seabed and becomes more discrete towards the surface. Generally, for velocities above 2m/s, TI is larger near the seabed, as expected. TI varies substantially both with distance above the seabed and stage of the tidal cycle.

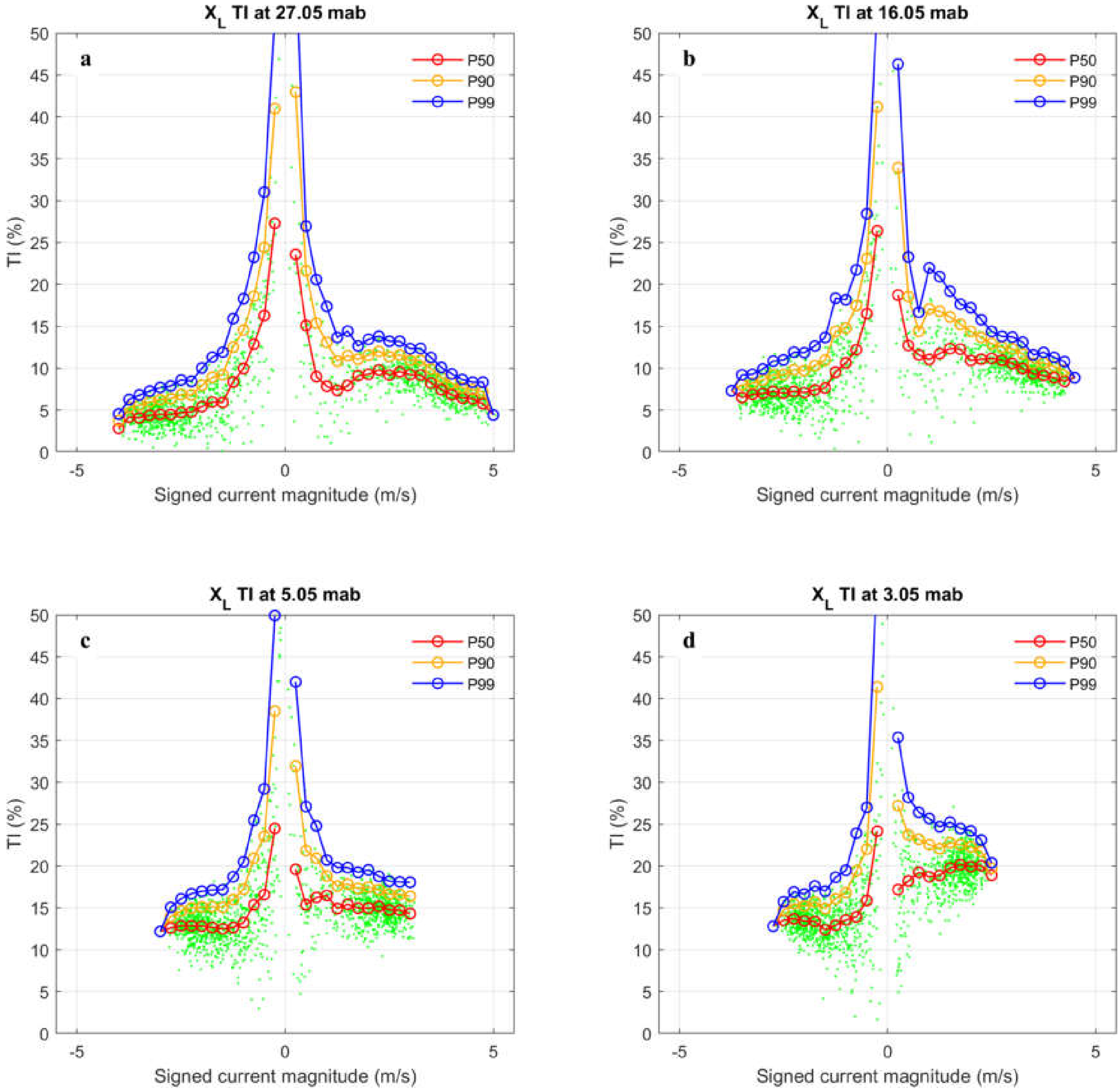

Figure 3 - 50th, 90th and 99th percentiles of TI along X_L axis

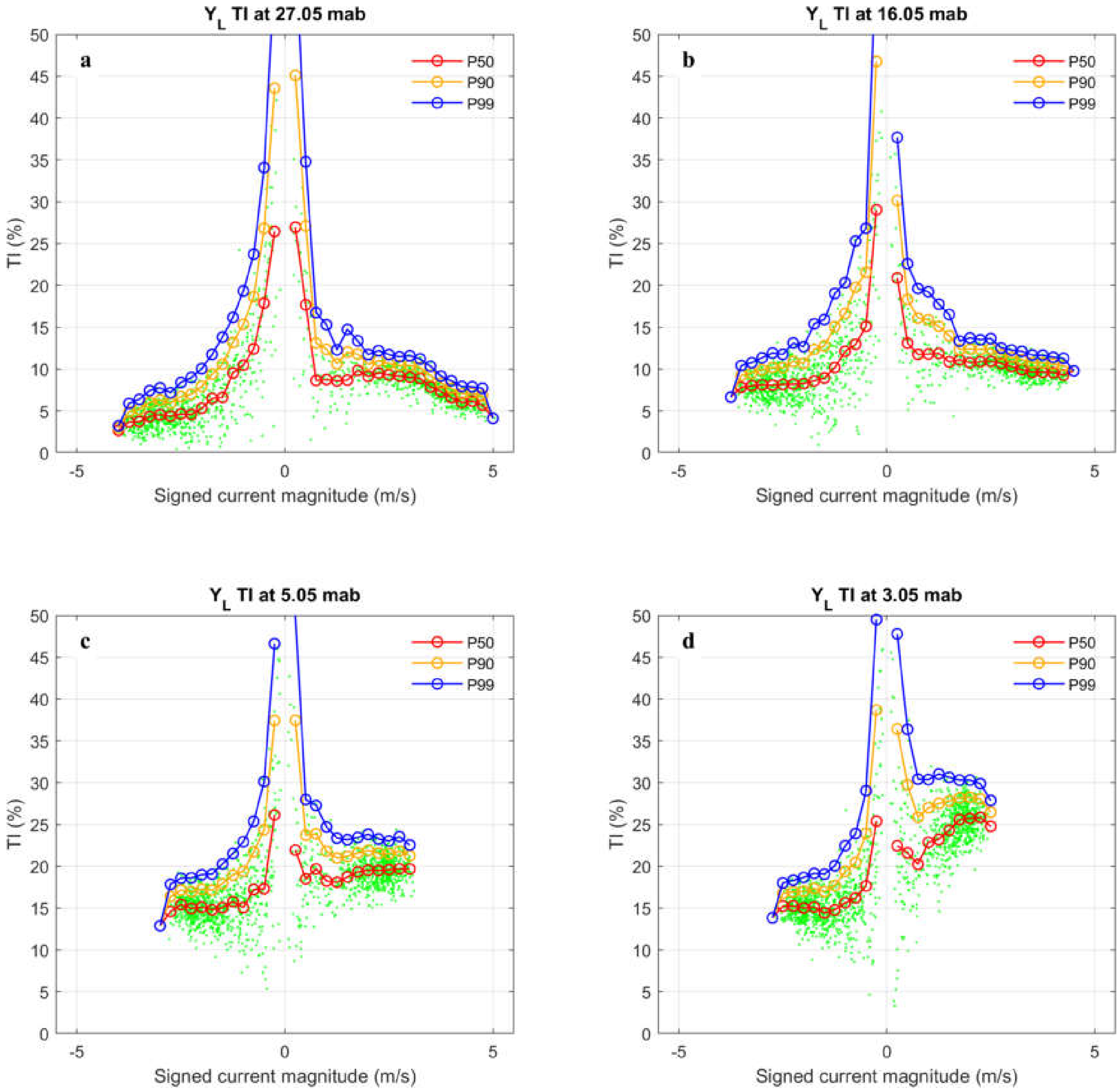

Figure 4 - 50th, 90th and 99th percentiles of TI along Y_L axis

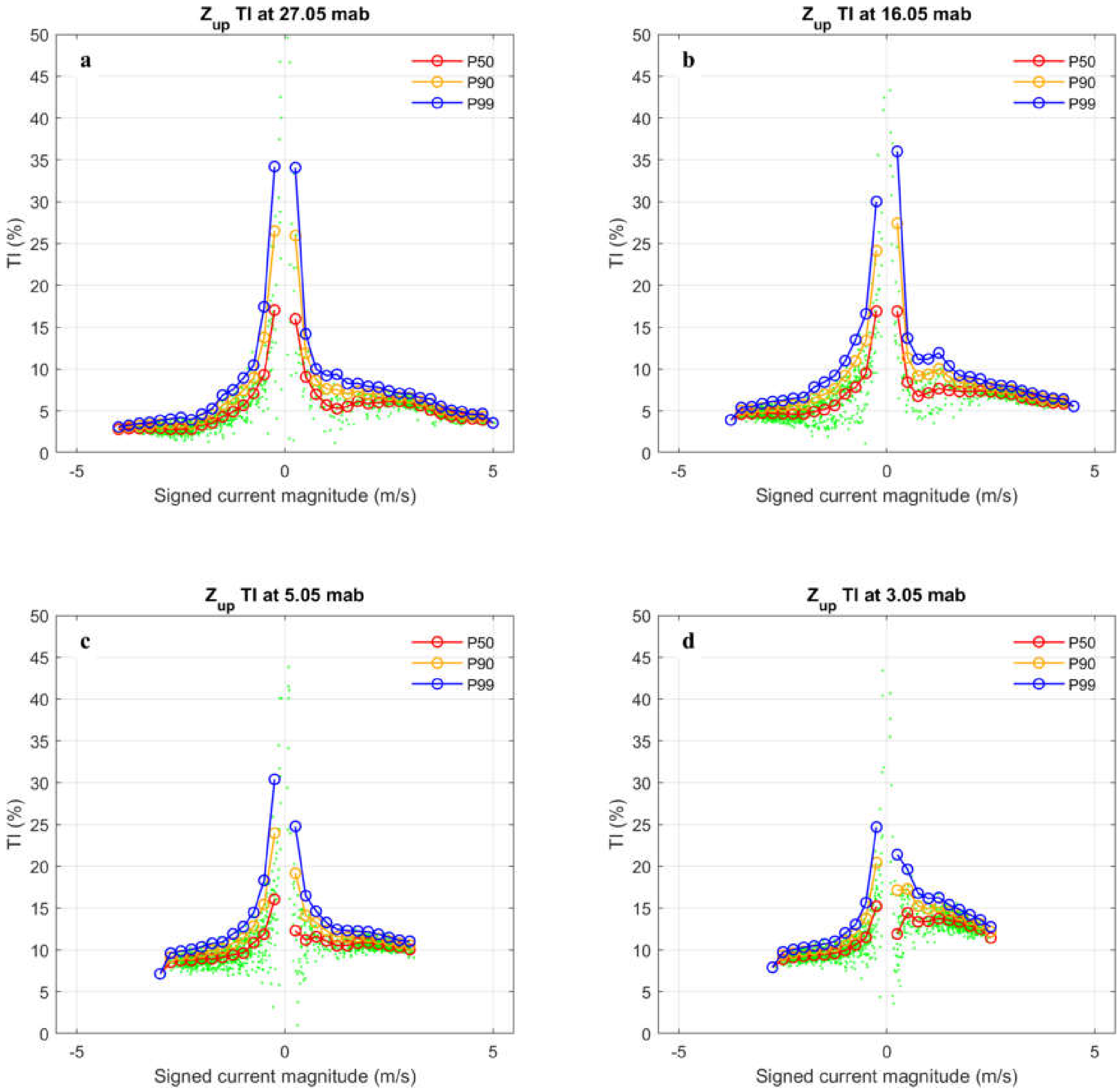

Figure 5 - 50th, 90th and 99th percentiles of TI along Zup axis

2.1.2.2 TI profile with height above seabed

Figure 6 provides TI profiles for current magnitude > 1m/s (and H_{m0} < 0.5 m). The profiles show the P50, P90 and P99 TI for current directions X_L, Y_L and Z_{up}. As discussed above, TI is larger near the seabed and gradually decreases towards the surface. The TI in the horizontal directions is greater than in the vertical direction.

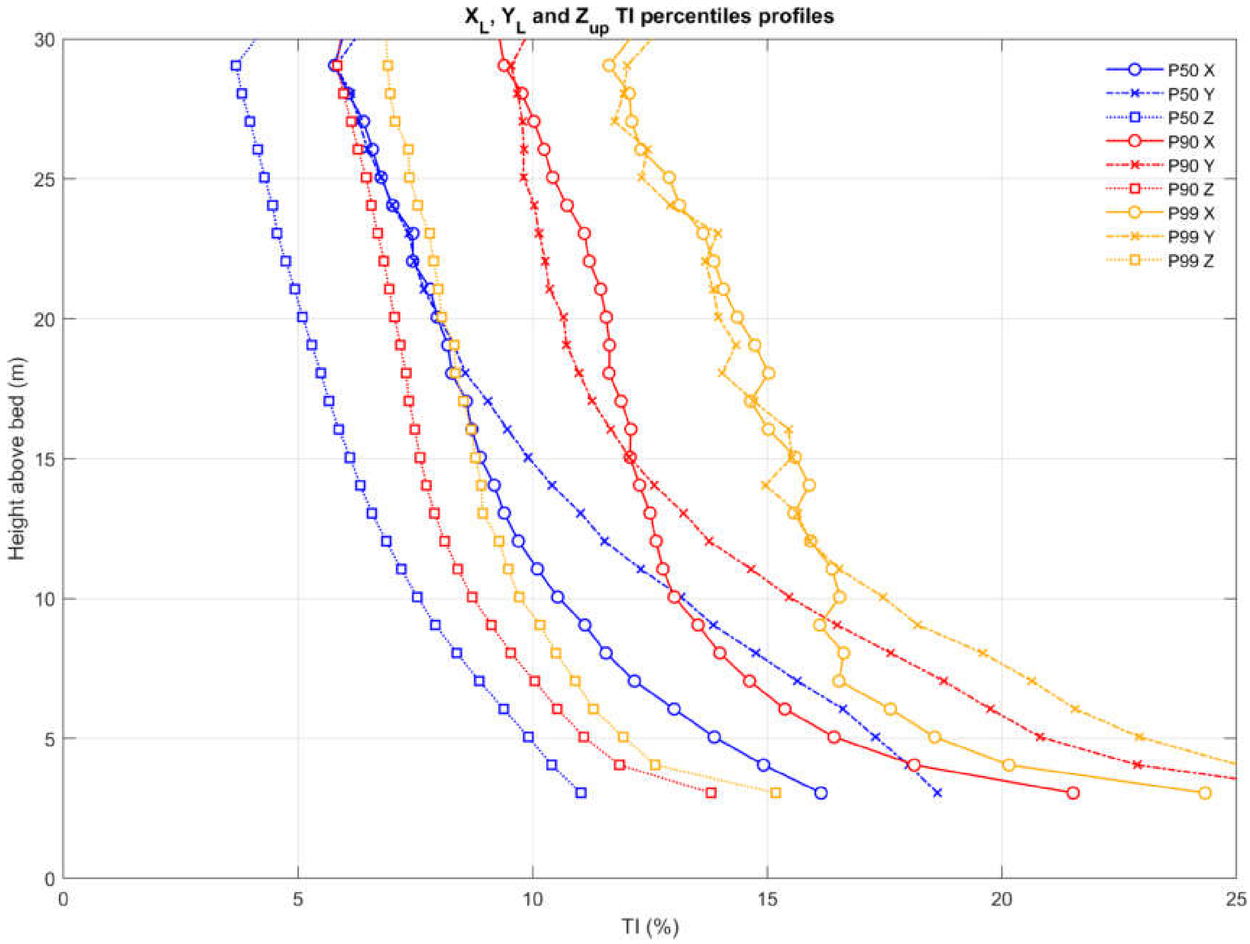

Figure 6 - 50th, 90th and 99th TI percentiles along X_L, Y_L and Z_{up} axes through the water column, for currents > 1m/s

2.1.2.3 TI using 4-beam method vs. 5-beam method

TI was also calculated using the 4-beam method, which is based on the standard deviations calculated directly from the instantaneous cartesian velocities. This is expected to be erroneous, since instantaneous cartesian velocities rely on the assumption of instantaneous flow homogeneity, which is systematically false in the presence of turbulence and waves. Although it is erroneous, the doppler noise variance has also been subtracted from the total variance for consistency. In this case, doppler noise was estimated from the levelled instrument velocity spectra.

As shown in Figure 7 and Figure 8, in the horizontal X_L and Y_L directions, the 4-beam method leads to an overestimation of TI, with various offsets that vary with distance above the seabed.

Contrastingly, as shown in Figure 9, in the vertical direction, the 4-beam method underestimates TI. This underestimation increases towards the surface.

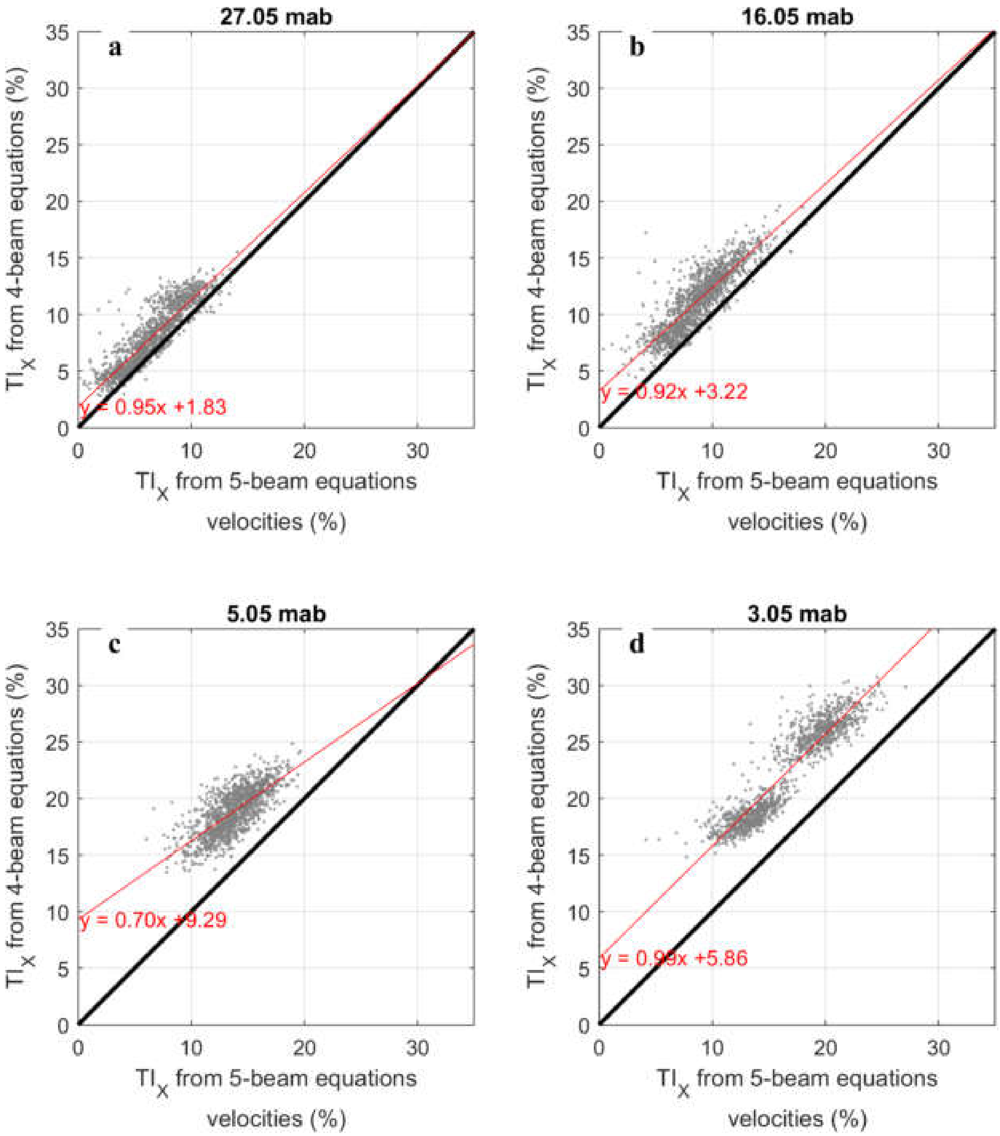

Figure 7 - Scatter plots of TI in the X_L direction using 5-beam equations against 4-beam equations for reference heights above seabed

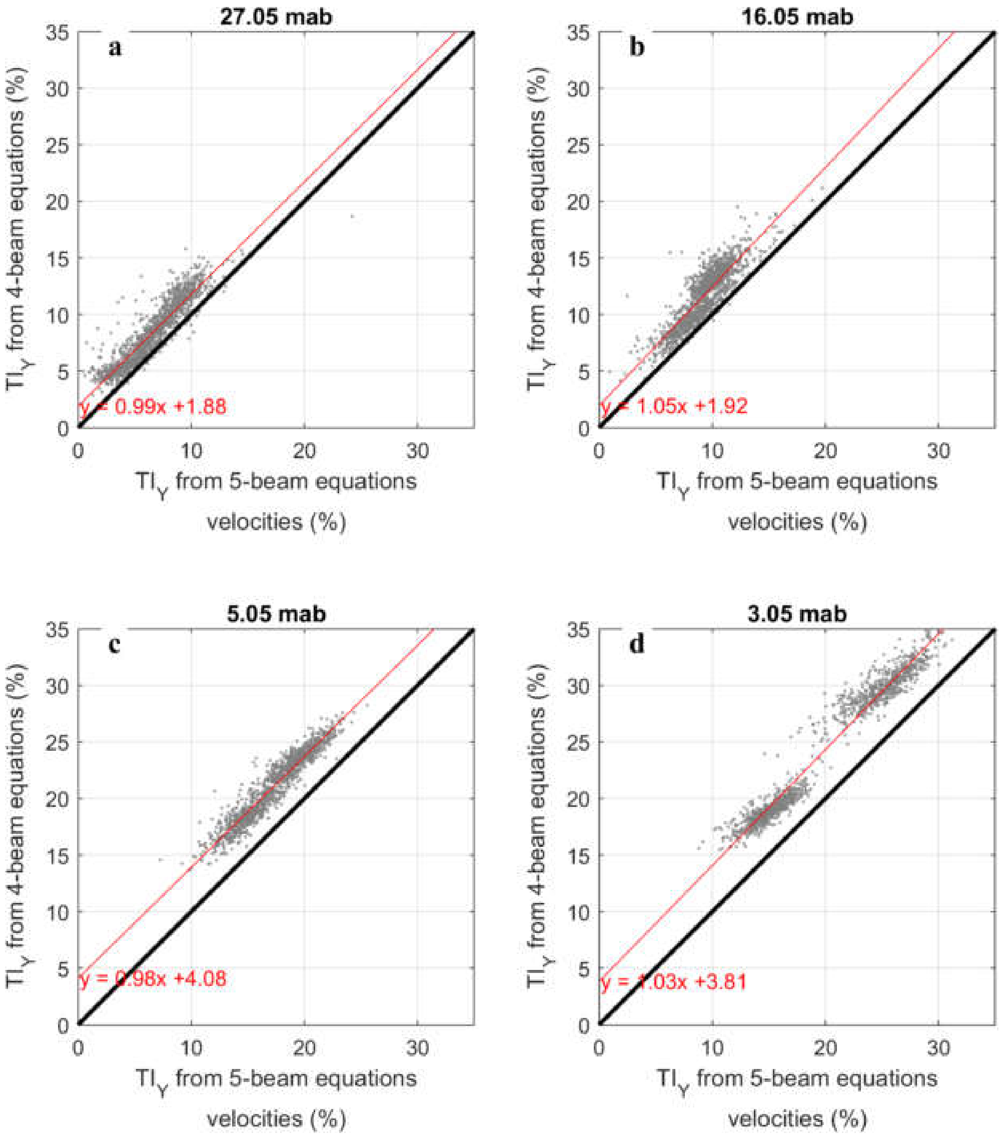

Figure 8 - Scatter plots of TI in the Y_L direction using 5-beam equations against 4-beam equations for reference heights above seabed

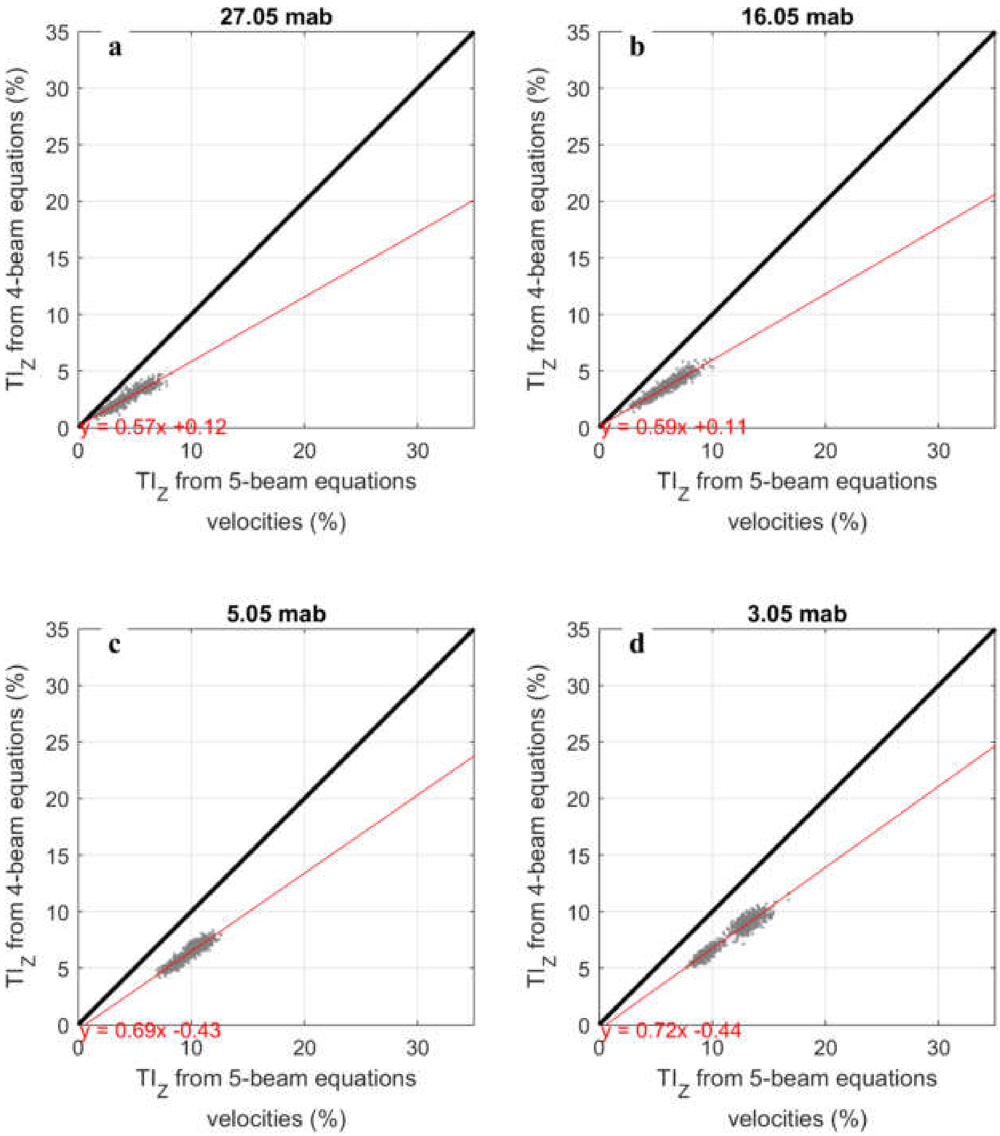

Figure 9 - Scatter plots of TI in the Z_{up} direction using 5-beam equations against 4-beam equations for reference heights above seabed

2.1.2.4 TKE profile with height above seabed

TKE was computed using the Reynolds stresses calculated from the 5-beam ADCP equations, as discussed above. In Figure 10, the mean TKE profile refers to time-averaged results, for current magnitude > 1m/s (and H_{m0} < 0.5 m). The P50, P90 and P99 percentiles were derived as for the TI.

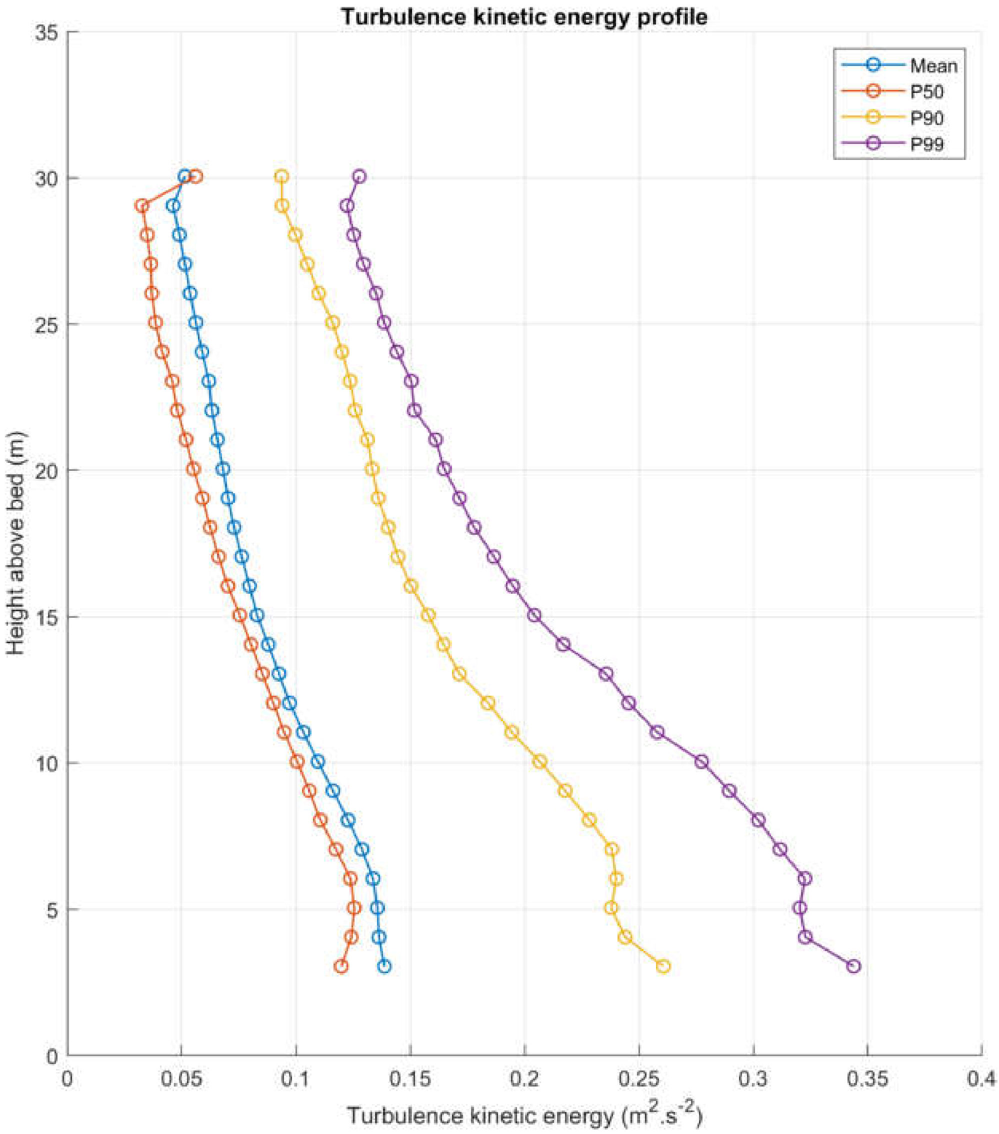

Figure 10 - Turbulence kinetic energy profiles split per percentile

2.1.2.5 TI using 4-beam method vs. 5-beam method

Similarly to TI, TKE was also calculated using the 4-beam method, which is based on the Reynolds stresses calculated directly from the instantaneous cartesian velocities. Comparing the 4-beam results with the reference 5-beam results in Figure 11 shows that the 4-beam method overestimates the TKE by c. 25-50% depending on the height above seabed.

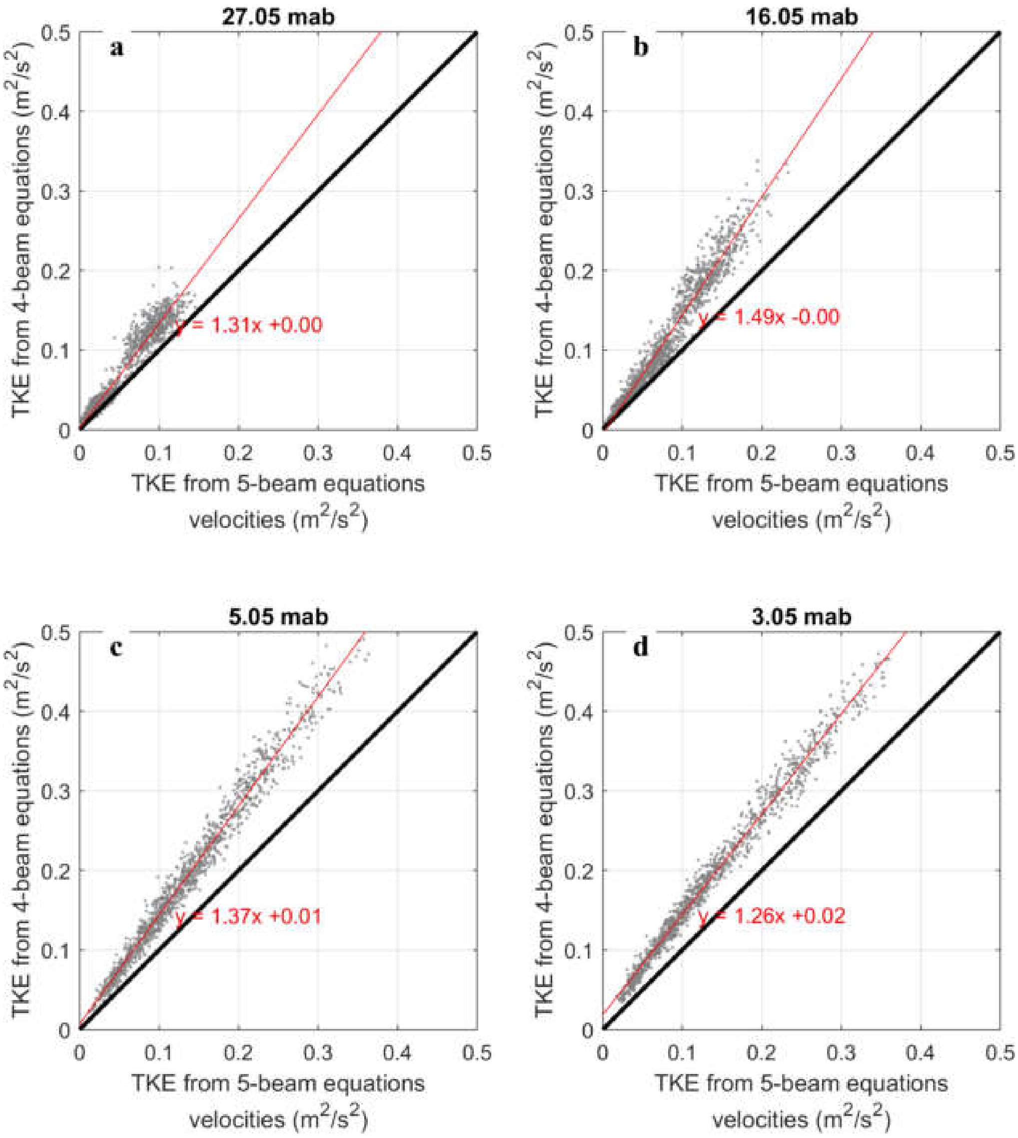

Figure 11 - Scatter plots of TKE established using 5-beam equations against 4-beam equations for reference heights above seabed

3 HIGH-FIDELITY VMADCP MEASUREMENTS AND DATA ANALYSIS

As discussed in Section 0, the high-fidelity VMADCP measurements were to:

- Undertake measurements of wake development and dissipation from existing MeyGen turbines, and provide the results of the wake measurements to allow the industry to calibrate and validate mathematical modelling of an operational turbine wake;
- Undertake measurements at potential future tidal turbine locations for array development/optimisation.

High-fidelity VMADCP data sets were collected at 1Hz, using a Teledyne Workhorse Monitor 600kHz ADCP, configured for 50 depth cells each of 1m. All IEC TS 620600-201 requirements relevant to VMADCP deployments were met or exceeded.

These data sets include data associated with the following survey approaches:

- ‘stationary’: almost-stationary data collection for long continuous periods (> 1 hour), intended to test the period of time needed for representative stopover data.
- ‘stopover’: as discussed in Section 0, almost-stationary data collection for short periods (typically c. 5-7 minutes), generally repeated every hour for c. 12 hours (i.e., for a full 12 hour flood/ebb tidal cycle), to be (later) correlated to the concurrent long-term SMADCP data, with the intent that the resulting correlation could be used to predict the long-term flow occurrence at each stopover location.
- ‘wake drift’: data collection whilst the vessel with the VMADCP was drifting in the wake of an operational 18m diameter 1.5MW rated tidal turbine.
- ‘wake drive-up’: data collection whilst the vessel with the VMADCP was driving up the wake of an operational 18m diameter 1.5MW rated tidal turbine. This approach was also combined with stopover surveys in the wake (and also with the turbine switched between operational and non-operational states).
- ‘wake transect’: repeated transect surveys across the wake of an operational 18m diameter 1.5MW rated tidal turbine. This approach was used with the turbine switched between operational and non-operational states.

The remainder of this section describes the high-fidelity measurements and results.

3.1 Stationary data collection trials

The vessel and VMADCP was positioned for over two hours over an operational 18m diameter 1.5MW turbine, which has an onboard turbine-mounted ADCP (TMADCP). The TMADCP is upwards facing and the TMADCP data is immediately available via the MeyGen control system.

Data analysis was conducted using averaging periods of 5 minutes, 10 minutes, and 15 minutes - to investigate the period of time needed for representative stopover data.

The comparative analysis resulted in the stopover surveys being defined with a minimum of 5 minute stopovers.

This approach, and the accuracy of using VMADCP data when compared to SMADCP data, was later validated by similar stationary data collection and analysis over the SMADCP, see Section 3.7.2.

3.2 Stopover data collection trials

Stopover surveys were undertaken over two operational 18m diameter 1.5MW turbines (each with different designs/manufacturers), which have onboard TMADCPs as discussed above.

Example results from one of these trials is shown in Figure 12 (showing the area used in the data analysis) and Figure 13 (showing a comparison between the VMADCP stopover data and that from the TMADCP at 12m below LAT (chart datum, CD).

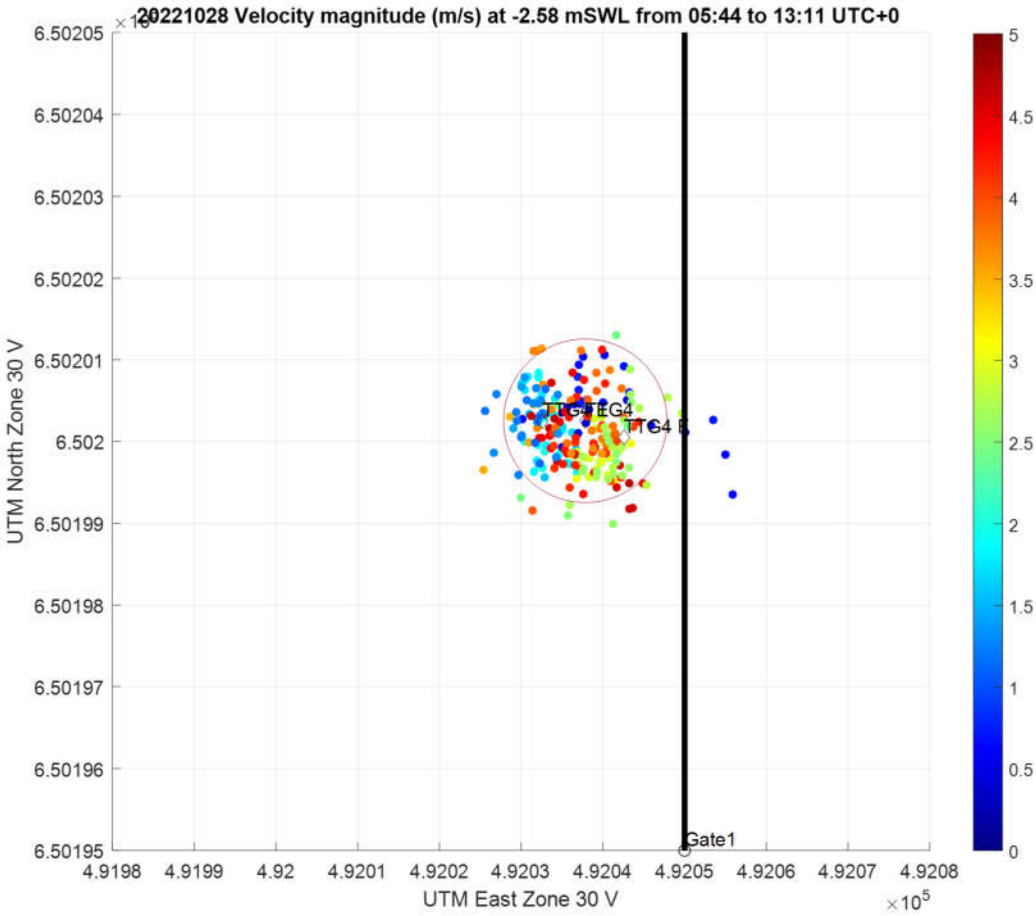

Figure 12 - Definition of area around TTG4 used in the data analysis

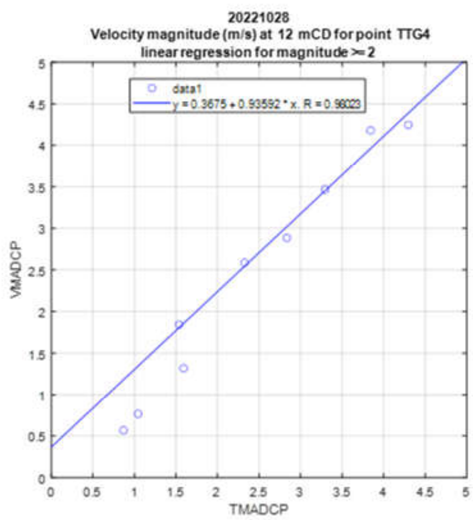

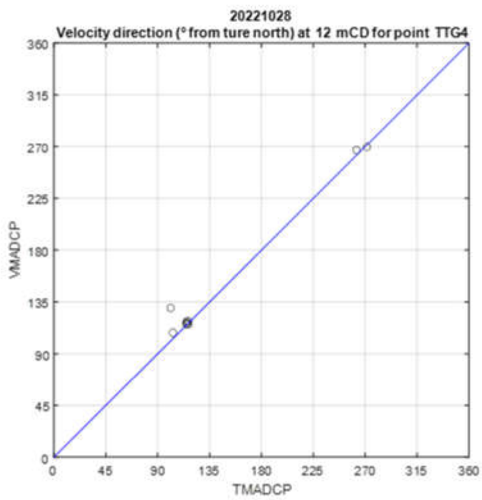

Figure 13 - VMSDCP and TMADCP data comparison for TTG4 stopover trial

3.3 Wake drift measurement results

As discussed in the introduction to Section 3, wake drift measurements refer to VMADCP data sets in which the vessel (and VMADCP) was drifting with the current along the wake, downstream of an operational 18m diameter 1.5MW rated turbine, whilst continuously collecting data.

Results of the horizontal current magnitude against depth and distance from the turbine (positive is downstream of the turbine) are shown for different stages of the tide, for two different turbines, in Figure 14 to Figure 17.

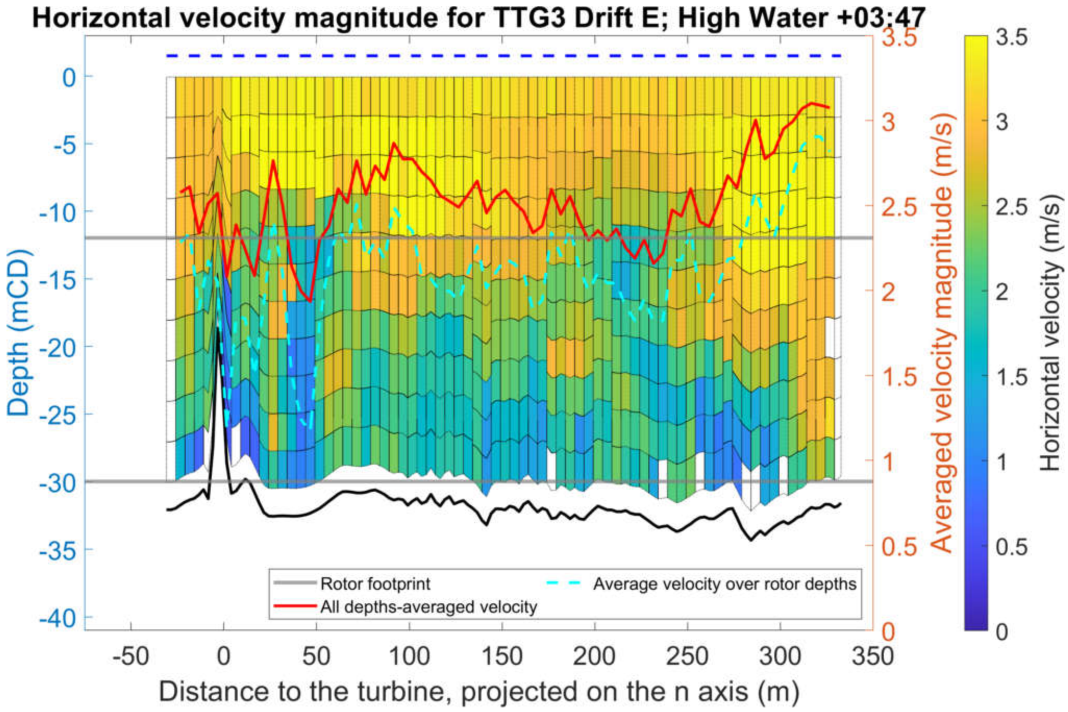

Figure 14 – Wake drift on TTG3

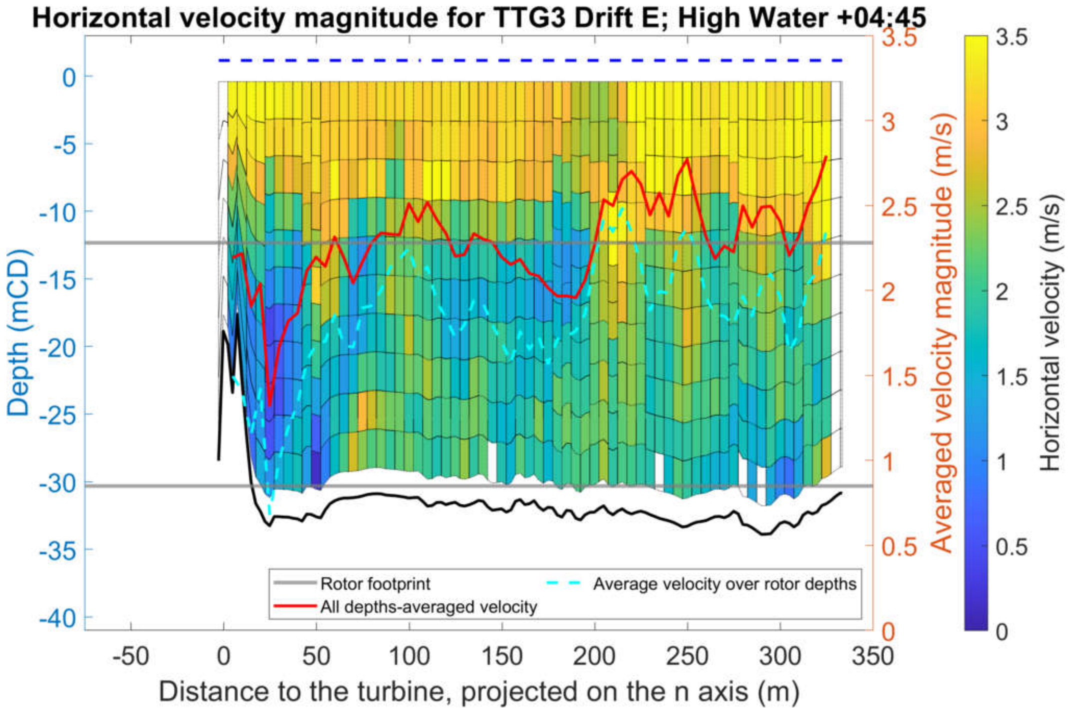

Figure 15 – Wake drift on TTG3

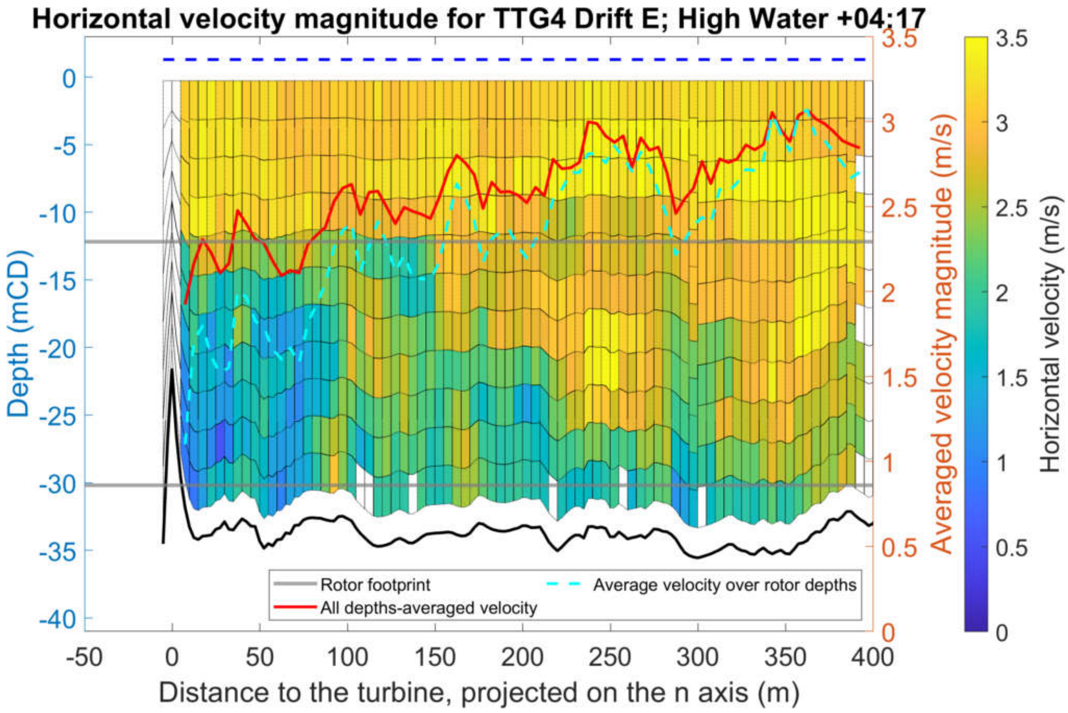

Figure 16 – Wake drift on TTG4

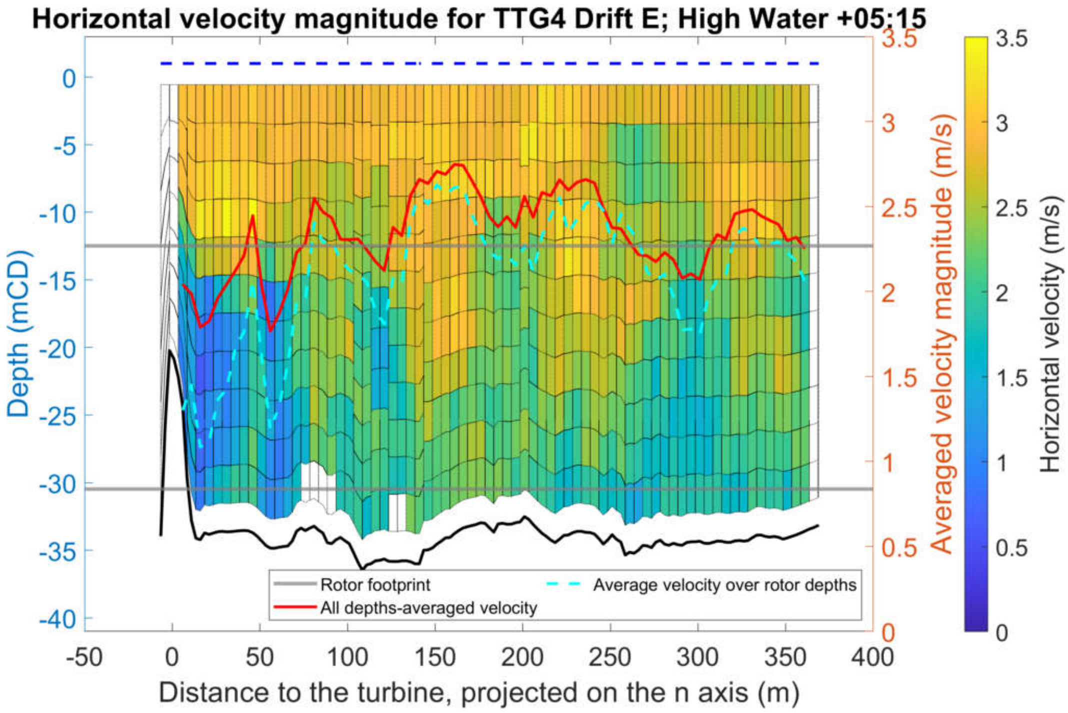

Figure 17 – Wake drift on TTG4

3.4 Wake drive-up measurement results

As discussed in the introduction to Section 3, wake drive-up measurements refer to VMADCP data sets in which the vessel (and VMADCP) was driving up against the current along the wake, downstream of an operational 18m diameter 1.5MW rated turbine, whilst continuously collecting data. Driving upstream, as opposed to drifting downstream, allows the VMADCP to collect more data, as the vessel can move more slowly. The drive-up measurements were generally taken from c. 14

turbine diameters downstream of the turbine to c. 4 diameters upstream (i.e., +14D to -4D). Results of the horizontal current magnitude against depth and distance from the turbine (positive is downstream of the turbine) are shown in Figure 18 and Figure 19. Velocity deficits compare the velocity at a location to the average velocity across the reference area shown.

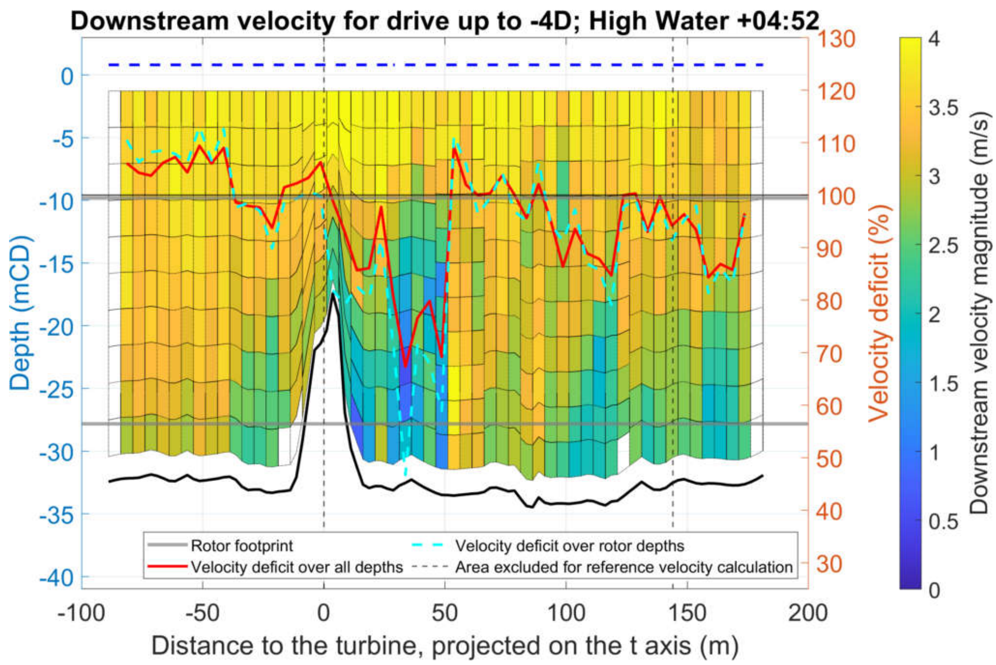

Figure 18 – Wake drive-up (ebb tide)

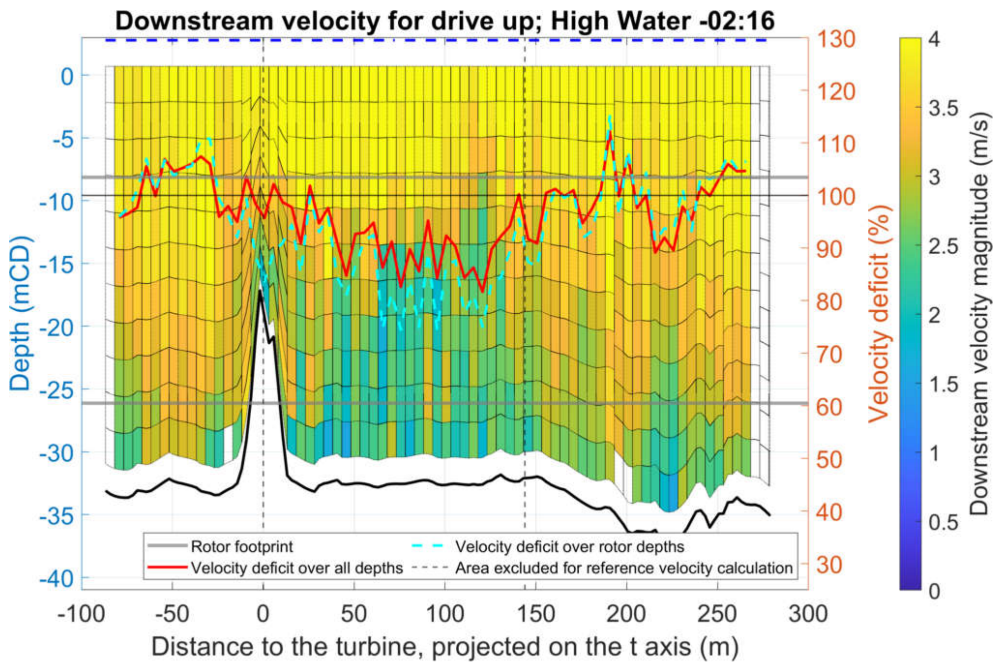

Figure 19 – Wake drive -up (flood tide)

3.5 Wake transect measurement results

As discussed in the introduction to Section 3, wake transect measurements refer to VMADCP data sets in which the vessel (and VMADCP) was driving across the wake, at various distances downstream of an operational 18m diameter 1.5MW rated turbine, whilst continuously collecting data.

The wake transects were planned to be repeated (at the same distance downstream of the turbine) a number of times in order to obtain satisfactory results (e.g. though elimination of instantaneous turbulence impacting the results).

3.5.1 Assessment of the required number of repeat wake transects

Initial trials were used to investigate the number of repeat transects required for satisfactory results, as the greater the number of repeat transects the fewer the number of different transects that could be achieved within a particular part of the tidal cycle. The final number of repeat transects was determined from review of velocities, covariances and a convergence analysis based on the maximum number of repeated transects (which was 7 repeat transects in the initial trials). As shown in Figure 20 and Figure 21, velocity reduction in the turbine wake is observed from the first transect and visually converges after 4 transects. Convergence was close to 100% across a large portion of the cross-section from 5 transects. Based on these results, later measurements were conducted using 5 repeat transects. These results are based on transects at +8D. The turbine rotor is at a depth of c. -12m to -30m.

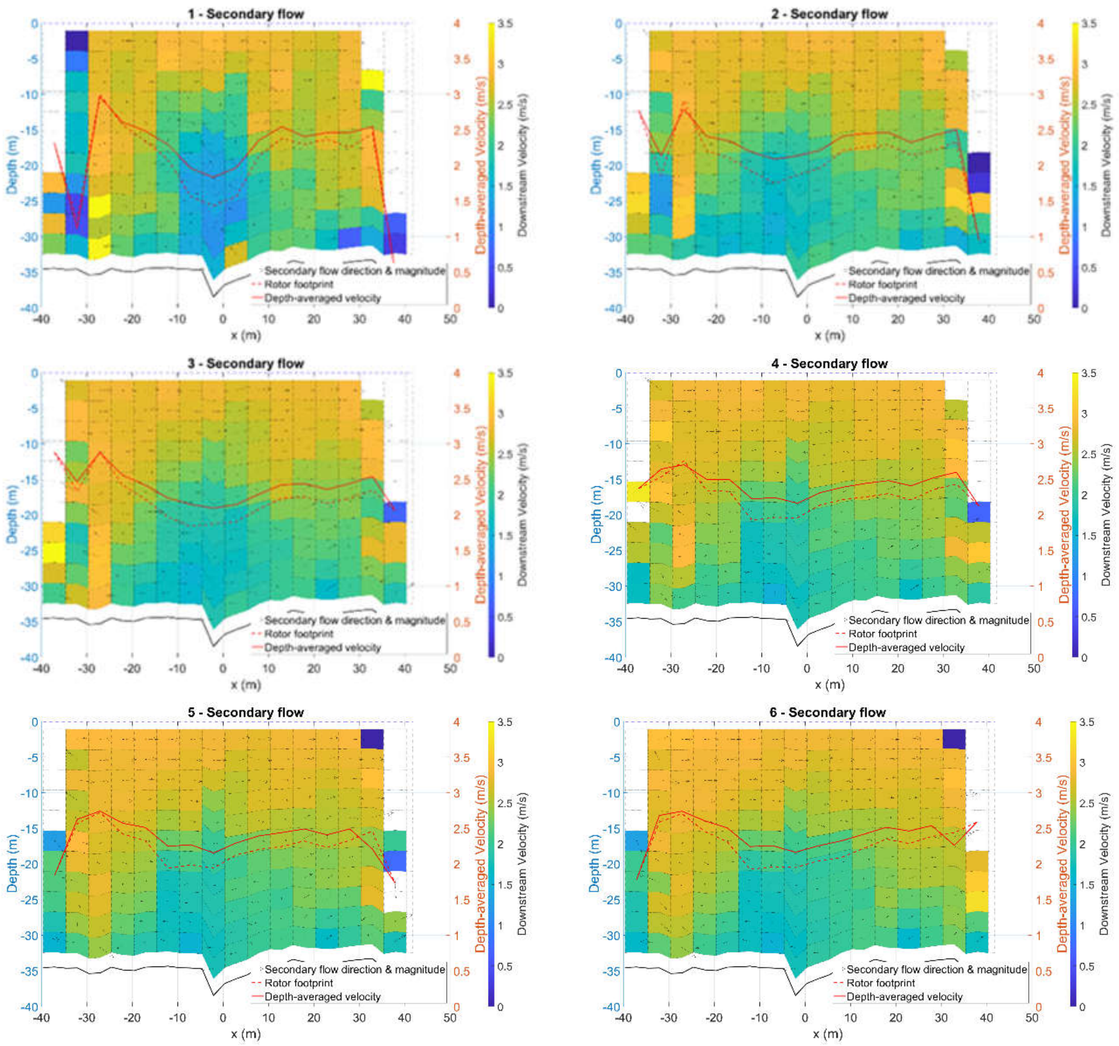

Figure 20 – Downstream velocity estimates from repeated transects in turbine wake

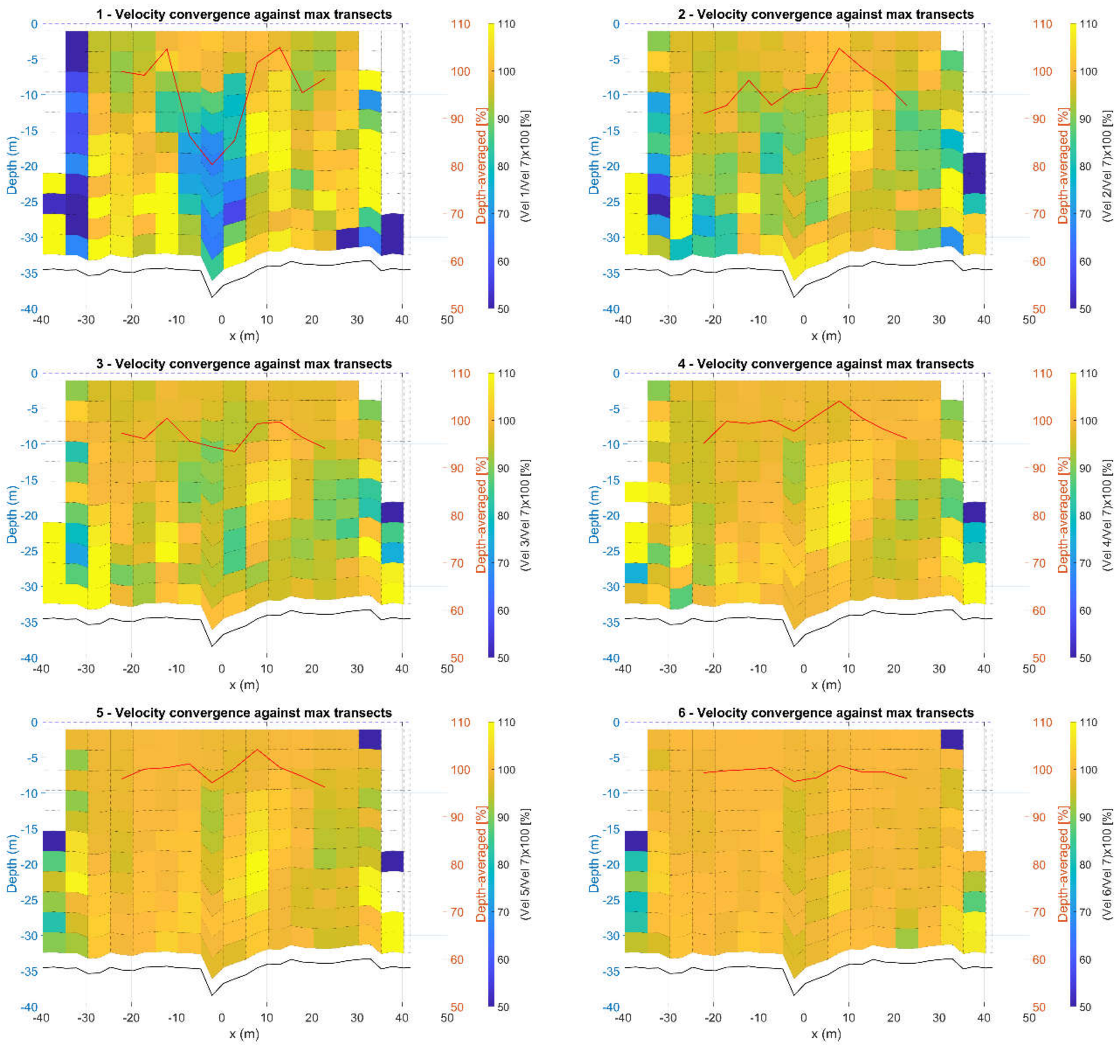

Figure 21 – Downstream velocity convergence from repeated transects in turbine wake

3.5.2 Results from repeated wake transects

Various methods to conduct the assessment of wake impacts from the repeated transects were investigated.

Initially, 5 repeat transects (as discussed above) were completed at various distances from an operational 18m 1.5MW tidal turbine, these distances being -2D, 0D, +2D, +4D, +6D, +8D, +9D, +10D, +11D, +12D (where D is the turbine diameter and positive is downstream of the turbine), with the turbine operational and switched off. Due to the time taken to undertake this number of transects, the velocity results for each set of repeat transects were scaled by the relevant velocity at the TMADCP.

A selection of the results is shown in Figure 22 to Figure 26.

In Figure 22, in flood tide and with the turbine off, the downstream velocity results show an element of randomness (likely due to high turbulence in flood tides at this location), which needs to be borne in mind when assessing Figure 23. However, Figure 23, with the turbine on, clearly shows the velocity reduction in the turbine wake when the turbine is switched on, with the wake clearly visible until 6-8D (averaged over all depths) and 9D (averaged over rotor depths).

In Figure 24, in ebb tide and with the turbine off, the downstream velocity results are reasonable consistent (e.g. vs. Figure 22). Figure 25 clearly shows the velocity reduction in the turbine wake when the turbine is switched on, with the wake clearly visible until around 9D (all depths) and around 11D (rotor depths). The impacts are perhaps even clearer when considering the velocity deficit, as shown in Figure 26. Velocity deficits compare the velocity at a location to the average velocity across the reference area shown.

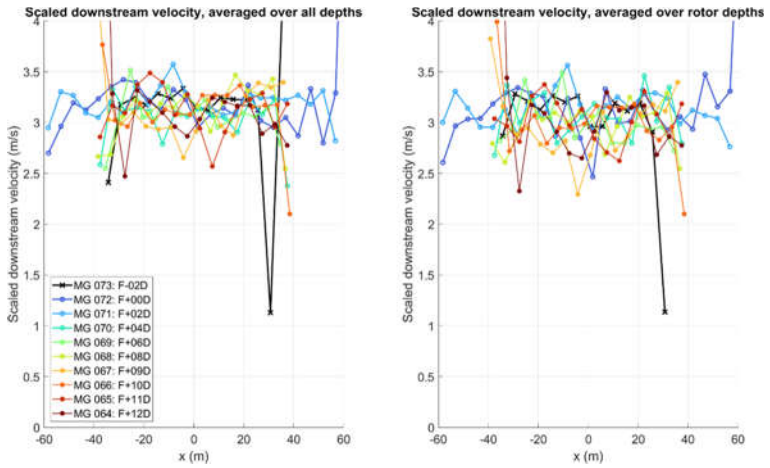

Figure 22 – Scaled downstream velocity, flood direction (turbine off)

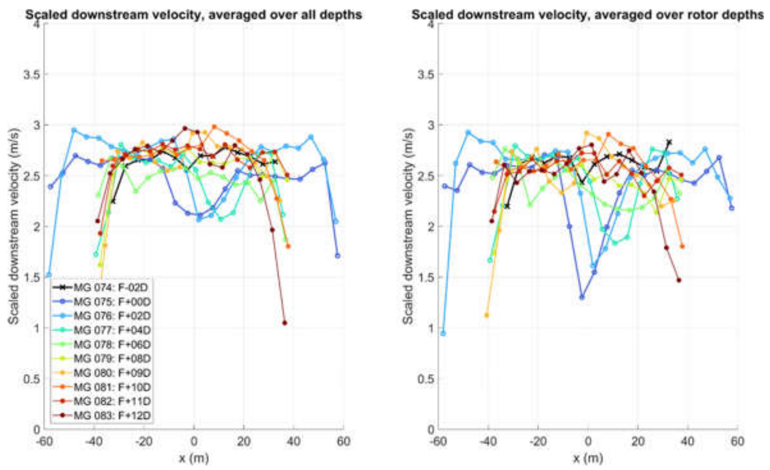

Figure 23 – Scaled downstream velocity, flood direction (turbine on)

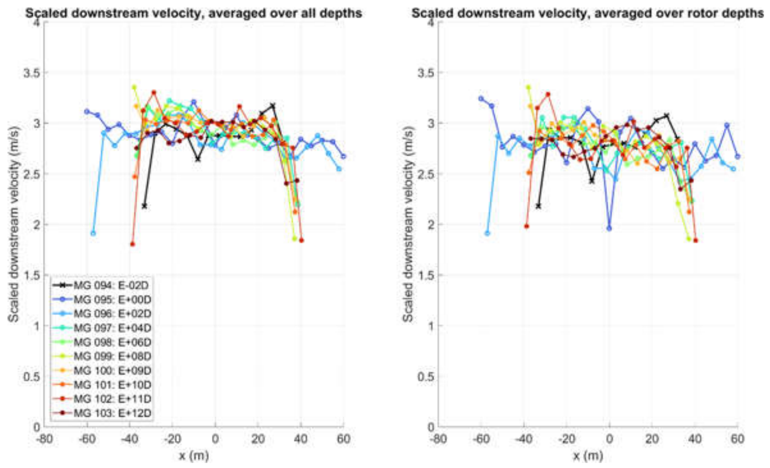

Figure 24 – Scaled downstream velocity, ebb direction (turbine off)

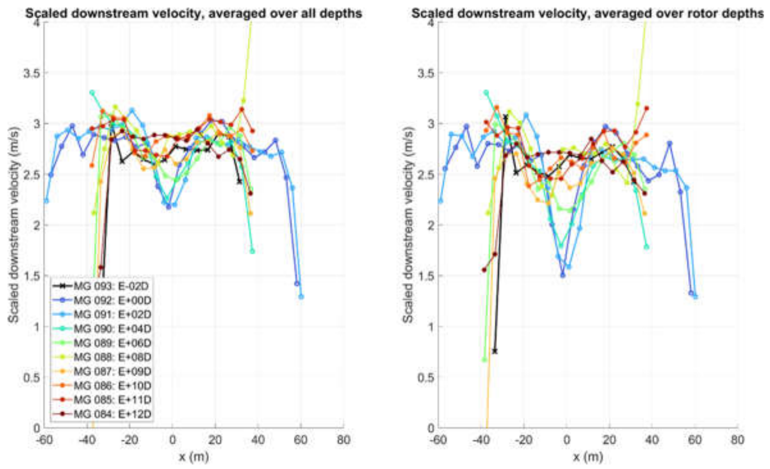

Figure 25 – Scaled downstream velocity, ebb direction (turbine on)

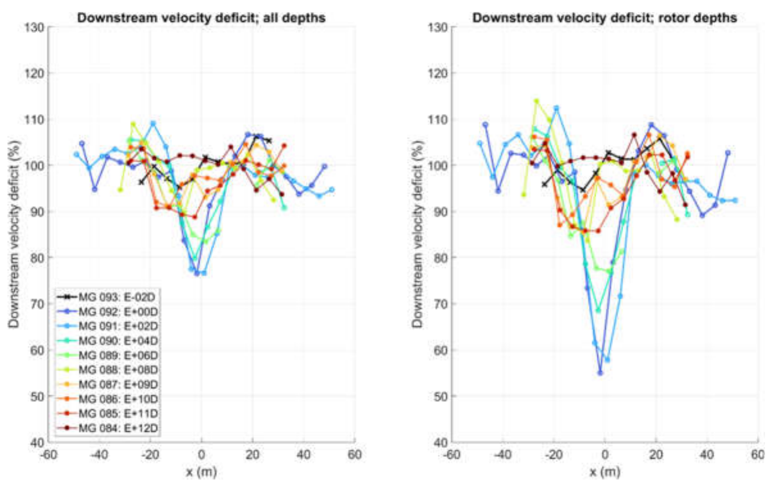

Figure 26 – Downstream velocity deficit, ebb direction (turbine on)

3.6 Wake stopover measurement results

The stopover approach, as discussed in Section 3.2, was also used to assess the wakes from operational 18m 1.5MW rated turbines.

Although there is only c. 10 minutes between the turbine on and off states, the current magnitude may change by up to c. 10% in this period. Therefore, as discussed in Section 3.5.2, the velocity results were scaled by the relevant velocity at the TMADCP. However, even though there is only c. 10 minutes between the turbine on and off states, this scaling introduces errors where there is a highly time-varying current, and hence only data were this scaling requirement was minor is considered.

This approach showed that the power-weighted depth-averaged velocity magnitude over the expected rotor disk area was reduced by c. 10% at +10D and by c. 5% at +14D. Figure 27 and Figure 28 show the scaled velocity magnitude and direction profiles with depth. Wake stopover measurements were not conducted closer to the turbine than 10D.

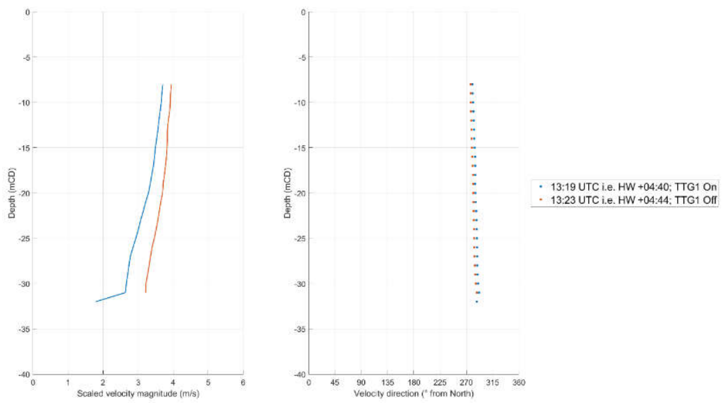

Figure 27 – Scaled velocity magnitude and direction at +10D (ebb)

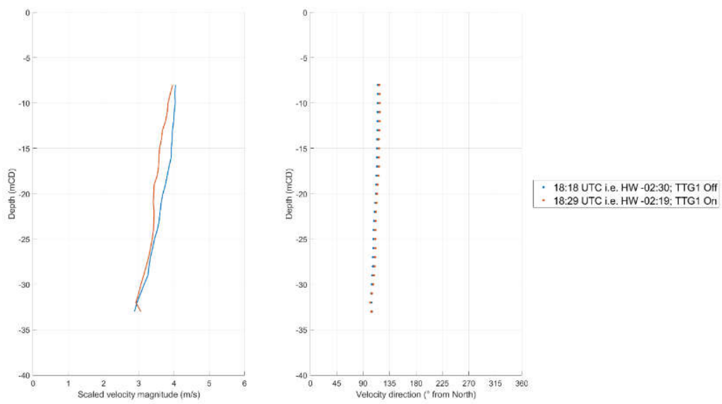

Figure 28 – Scaled velocity magnitude and direction at +14D (flood)

3.7 Resource assessment using combined stopover VMADCP and SMADCP data

As discussed in the introduction to Section 3, and based on the trials outlined in Section 3.2, further stopover VMADCP measurements were undertaken at potential future tidal turbine locations, and then correlated to the concurrent long-term SMADCP data to predict the long-term flow occurrence at each stopover location for array development/optimisation.

3.7.1 Time lag investigation

Initially, an investigation into the potential time lag of the currents between the potential future tidal turbine locations and the SMADCP location was undertaken, to assess whether a time lag was required in the correlation between the VMADCP data and the SMADCP data. Rather than conduct this between VMADCP and SMADCP data, when the VMADCP data was only collected at the same position every c. 1 hour, this investigation compared the SMADCP data to the TMADCP data at one of the existing MeyGen tidal turbines (which was positioned at a similar distance to that of the proposed tidal turbine locations most distant from the SMADCP).

The investigation used a 10-minute moving average of the 1-minute TMADCP and SMADCP averaged data, to minimise the effects of short-term fluctuations, and reviewed the time of tidal velocity peaks and current reversal, as well as the overall time lag through cross-correlation of the velocity time series data (via time shifting). The investigation was conducted using a 7-day period of relatively calm weather (to minimise pressure effects).

Even with the moving average to reduce the influence of local peaks in the currents, the time lag between individual peaks still varied, reaching 22 minutes in one case during ebb tides, but remaining below 8 minutes in most cases. Which ADCP reached peak velocity first also varied, with the sign of the time lag varying as a result. The average time lag during flood and ebb tides was only around 1 minute.

The maximum time lag obtained for current reversals was 11 minutes, The average time lag was c. 5 minutes.

When considering the overall time lag through cross-correlation of the velocity time series data (via shifting one set of data by a series of 1-minute intervals), it was found that maximum cross-correlation between the TMADCP and SMADCP data sets was achieved with zero time lag.

Therefore, the later correlations of VMADCP to SMADCP measurements used no time lag correction.

3.7.2 VMADCP vs SMADCP correlation at SMADCP location

As discussed in Section 3.2, initial stationary trials were conducted by comparing VMADCP measurements to TMADCP measurements at an existing tidal turbine, and the approach was then later validated by similar stationary VMADCP data collection and analysis over the SMADCP – as discussed in this section. The VMADCP and SMADCP measurements were conducted at different frequencies to avoid any interference issues.

3.7.2.1 Data selection

VMADCP data to be compared with SMADCP was selected using the vessel position coordinates. All data points recorded within a target circle, centred at the SMADCP location and with a c. 10 metre radius, were included.

Data selection is shown in Figure 29. The position of the VMADCP during its stationary measurements is plotted as grey lines. The black cross indicates the position of the SMADCP, and the black circle shows the circumference of the target circle. The vessel pilot endeavoured to keep the VMADCP on the vessel within the target circle. The red dots indicate the data points that were retained for the analysis.

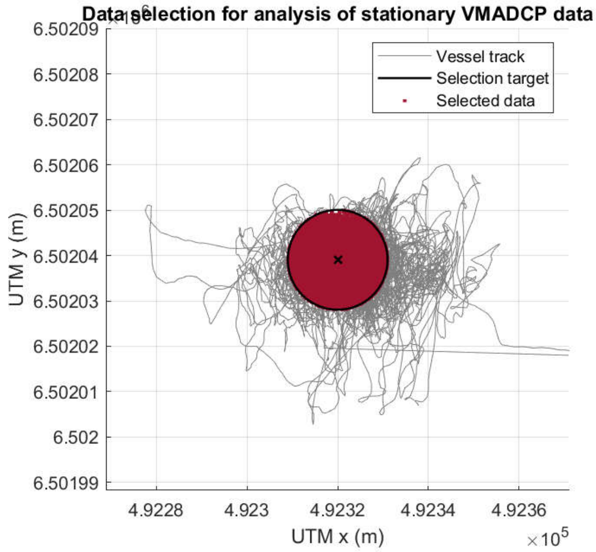

Figure 29 – Vessel tracks for VMADCP data over SMADCP location and target location

3.7.2.2 Data analysis

A linear regression fit was applied at each depth cell to evaluate the correlation between velocity magnitudes from both data sets using 10-minute averaged data, with the linear regression forced through the origin, and only considering velocity magnitudes from both VMADCP and SMADCP that were higher than 1m/s.

The power-weighted depth-averaged velocity magnitude over the expected rotor disk area was also computed, commonly referred to as the “method of bins” (IEC TS 62600-200, 2013)[3].

3.7.2.3 Results

The results show a very strong correlation between the velocity magnitudes from the VMADCP data at the SMADCP location and the actual SMADCP data.

Linear fits have R coefficients above 0.99 at all turbine-relevant depths except for 30m below LAT and deeper. Angular coefficients are very close to 1 and only small offset values were found.

Around hub height, the linear fit is extremely good, as an example see Figure 30 and Figure 31, which show the VMADCP measurements of velocity magnitude on average match the SMADCP data to within < 1%, including for the power-weighted depth-averaged velocity magnitude over the expected rotor disk area.

[3] Marine energy – Wave, tidal and other water current converters – Part 200: Electricity producing tidal energy converters – Power performance assessment. Edition 1.0. 2013-05. See: https://webstore.iec.ch/preview/info_iec62600-200%7Bed1.0%7Den.pdf

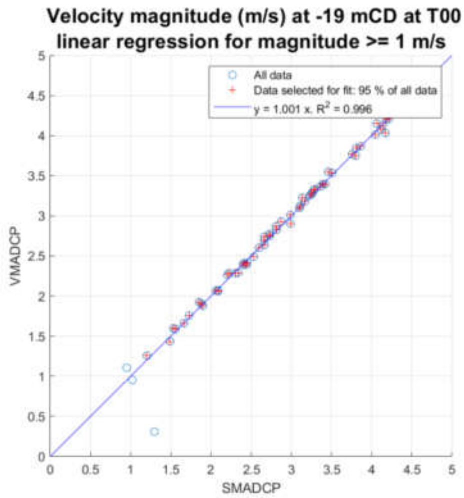

Figure 30 – Linear regression of VMADCP vs SMADCP data at 19m below LAT (stationary data)

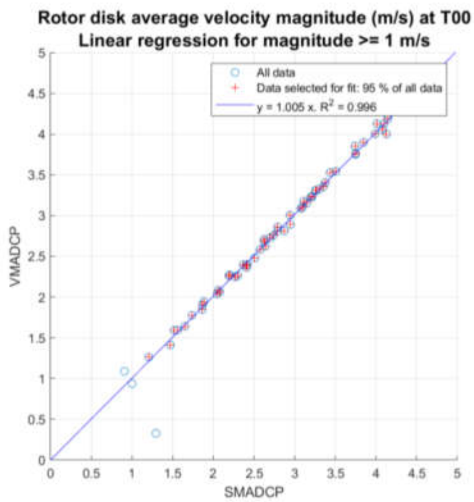

Figure 31 – Linear regression of VMADCP vs SMADCP data for rotor disk (stationary data)

3.7.3 VMADCP vs SMADCP correlation at potential turbine locations

Based on the results of the stationary and stopover trials discussed above, VMADCP data was then collected using the stopover technique at over 10 potential future tidal turbine locations, as well as over the SMADCP and near several of the existing tidal turbines. The stopover duration of 5-7 minutes at each location was maximised within the constraints of the number of locations to be returned to every hour and the number of days available for the survey.

Data selection and analysis was as discussed in Section 3.7.2.1 and 3.7.2.2, except that the duration of the stopovers varied at the various locations as discussed above.

3.7.3.1 Results

The quality of the fit depends largely on the distance of the potential turbine location from the SMADCP location.

At the VMADCP stopovers over the SMADCP location, for the power-weighted depth-averaged velocity magnitude over the expected rotor disk area, the R coefficient was slightly lower than for the stationary survey outlined in Section 3.7.2, being 0.992 vs 0.998, and the angular coefficient was 1.009 vs 1.005; see Figure 32.

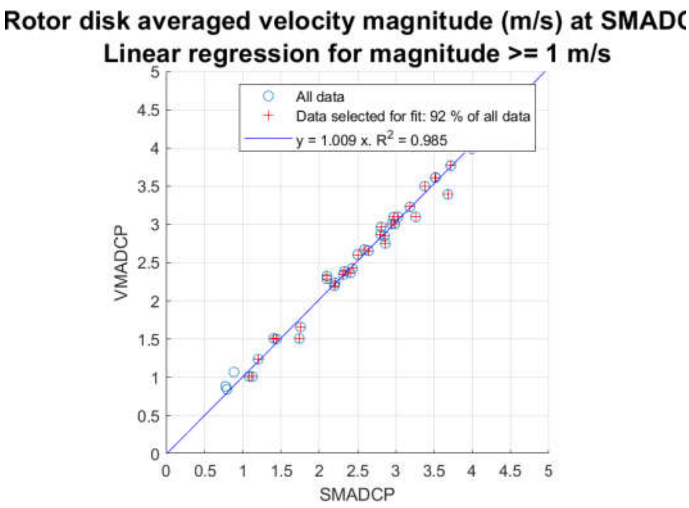

Figure 32 – Linear regression of VMADCP vs SMADCP data for rotor disk (stopover data)

For the potential turbine locations less than 200m away from the SMADCP, R values were on average > 0.97. See Figure 33 for an example of such a potential turbine location.

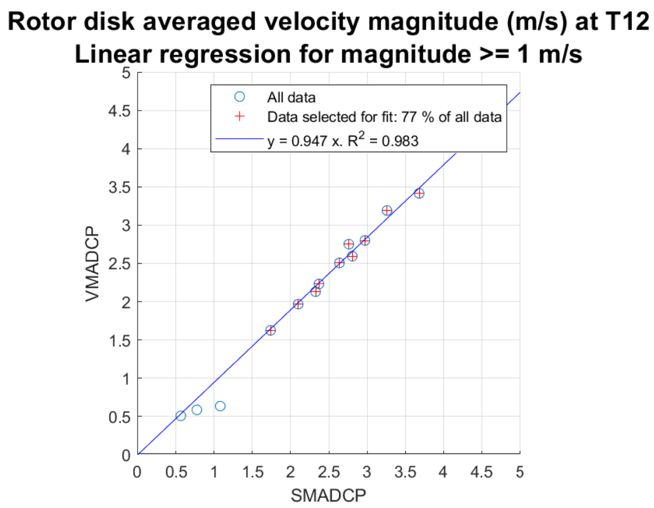

Figure 33 – Linear regression of VMADCP vs SMADCP data for rotor disk (stopover data)

R coefficients were still above 0.95 for potential turbine locations up to c. 500m away from the SMADCP, and beyond that the reason for some lower R values may be related more to shear lines in the flow rather than solely distance.

3.7.3.2 Conclusions

The results generally show a very strong correlation between velocity magnitudes from the VMADCP data at the potential turbine locations and the SMADCP data (with R values generally 0.95-1.00), providing high confidence in the technique's applicability.

Combined with MeyGen's existing knowledge of the site through other measurements and hydrodynamic modelling undertaken since c. 2010, MeyGen has used the results of the innovative stopover approach combined with the SMADCP to determine the long-term tidal resource at potential future tidal turbine locations for use in its project development. Due to the success of the approach, no further hydrodynamic modelling is planned in the short-term.

MeyGen has already approached the IEC TS 62600-201 maintenance team to discuss its findings, and the approach is planned to be incorporated into future editions of the IEC TS 62600-201 technical specification. MeyGen, ARR and DO plan to disseminate further details of the approach at the EWTEC conference and papers in September 2023.

TIGER TIDAL STREAM INDUSTRY ENERGISER

EUROPEAN UNION
European Regional Development Fund